

Ultra High Pressure Hydrogen Studies

by

Andrew Richard Schicho

Department of Mechanical Engineering
Duke University

Date: _____

Approved:

[Nico Hotz], Supervisor

[Adrian Bejan]

[Helen Hsu-Kim]

[Walter Neal Simmons]

Dissertation
Pratt School of Mechanical Engineering
Duke University
2015

Abstract

Hydrogen has been called the fuel of the future, and as it's non-renewable counterparts become scarce the economic viability of hydrogen gains traction. The potential of hydrogen is marked by its high mass specific energy density and wide applicability as a fuel in fuel cell vehicles and homes. However hydrogen's volume must be reduced via pressurization or liquefaction in order to make it more transportable and volume efficient. Currently the vast majority of industrially produced hydrogen comes from steam reforming of natural gas. This practice yields low-pressure gas which must then be compressed at considerable cost and uses fossil fuels as a feedstock leaving behind harmful CO and CO₂ gases as a by-product. The second method used by industry to produce hydrogen gas is low pressure electrolysis. In comparison the electrolysis of water at low pressure can produce pure hydrogen and oxygen gas with no harmful by-products using only water as a feedstock, but it will still need to be compressed before use. Multiple theoretical works agree that high pressure electrolysis could reduce the energy losses due to product gas compression. However these works openly admit that their projected gains are purely theoretical and ignore the practical limitations and resistances of a real life high pressure system. The goal of this work is to experimentally confirm the proposed thermodynamic gains of ultra-high pressure electrolysis in alkaline solution and characterize the behavior of a real life high pressure system.

Table of Contents

Abstract	5
List of Figures	9
Nomenclature	12
Acronyms.....	12
Acknowledgements	14
<i>1 Background</i>	15
1.1 Current Affairs.....	15
1.2 Alternative Fuels.....	17
1.3 Hydrogen Economy	20
<i>2 Introduction to Hydrogen</i>	23
2.1 Hydrogen as an energy carrier	23
2.2 Current hydrogen interest.....	26
<i>3 Electrolysis Methods And Theory In Literature</i>	28
3.1 Hydrogen Production By Electrolysis	28
3.1.1 Microbial Electrolysis.....	29
3.1.2 Photovoltaic Electrolysis	30
3.1.3 Solid Oxide Electrolysis.....	31
3.1.4 Polymer Electrolyte Membrane Electrolysis.....	32
3.1.5 Alkaline Electrolysis.....	33
3.1.6 Summary of State of the Art Technologies	35
3.2 Electrolysis Theory	36
3.2.1 Thermodynamics.....	36

3.2.2	Overvoltages and Efficiency	38
3.2.3	Pressurization.....	44
4.	Novelty	47
5.	Materials and Construction	49
5.1	Pressure Vessel System.....	49
5.1.1	Vessel.....	49
5.1.2	Top.....	51
5.1.3	Cap.....	54
5.1.4	Sub Vessel.....	55
5.1.5	Pump	59
5.2	Electrical System.....	59
5.3	Piping and flow system	61
6.	Experimental Procedures.....	63
6.1	Pressure safety testing	63
6.2	Electrical safety testing	63
6.3	Hydrogen Production Tests	65
7	Results and Discussion.....	68
7.1	System Design.....	68
7.2	Tap Water Testing	69
7.2.1	Stability Testing	69
7.2.2	Pressure Variation	72
7.2.3	Voltage Variation.....	76

7.3 Potassium Hydroxide Testing	79
7.3.1 Potassium Hydroxide Concentration Variation.....	79
7.3.2 Pressure Varriation.....	85
8 Conclusion	94
References	96

List of Figures

Figure 1: Impacts predicted to occur due to global climate change in five sections based on temperature increase. Affects will begin at temperature where the left of text is placed. Arrows indicate continued worsening conditions (IPCC 2007).	16
Figure 2: Electrical efficiency source to end use of BPV and FCV (Bossel 2006).....	19
Figure 3: A flow chart depicting a hydrogen based economy with integrated renewable and conventional electricity generation (Ball and Wietschel 2009).	22
Figure 4: Energy carrier densities. Hydrogen is seen far to the right. Energy densities vary in accuracy due to HHV and LHV discrepancies and pressurization.	23
Figure 5: Compressed hydrogen gas energy storage density <i>uv</i> vs. pressure source (Thomas and Keller 2003)	24
Figure 6: Microbial Electrolysis Cell courtesy of NSF (Deretsky 2012)	29
Figure 7: Diagram of a photovoltaic electrolysis cell (Zeng and Zhang 2010).	30
Figure 8: Solid Oxide Electrolysis Cell Source (Energy 2011).....	31
Figure 9: Polymer Electrolyte Membrane cell (Spurgeon and Lewis 2011).....	32
Figure 10: Alkaline Electrolysis Cell. Note that there is no need for a membrane in this type of cell but it can be added for increased gas purity.....	33
Figure 11: Predicted Reversible Electrolysis Voltage (Onda, Kyakuno et al. 2004)	37
Figure 12: Distribution of electrolysis cell voltage (Ohata 2009).....	38
Figure 13: Effect of electrode spacing on electrolysis efficiency (A-F.M. Mahrous 2011).40	
Figure 14: Conductivity of aqueous KOH vs concentration and temperature (R.J. Gilliam 2007, Frank Allebrod 2011)	40
Figure 15: Effect of KOH concentration on electrolysis efficiency (Ohata 2009).....	41
Figure 16: Energy demand of electrolysis vs temperature	43

Figure 17: Work for compression of 1 kg liquid water compared to work for compression of gases generated from 1kg of water. **Note that the scale for liquid compression (right) is 25 times smaller than the scale for the gas compression (left).....	45
Figure 18: Simplified, two-dimensional construction of pressure vessel. Does not include electrolysis components	49
Figure 19: Pressure Vessel, Fabricated by HIP according to our design and rated by ANSI for a working pressure of 5000 psi.....	50
Figure 20: Vessel Top Side view; 1: Thermowell, 2: Insulated internal electrode, 3: Buna N O-ring in groove, 4: Inlets/Outlets	51
Figure 21: Overhead view of pressure vessel top. Clockwise from 12 o'clock: Thermowell, positive electrode, flow outlet, flow inlet, negative electrode.	52
Figure 22: Technical drawing of a Conax gland for the electrode. Pressure rating from vacuum to 10,000 psi (Conax 2014).	54
Figure 23: Cap of the pressure vessel system with bore and threading shown.....	55
Figure 24: Flexible rubber diaphragm sub-vessel.	56
Figure 25: #60 Stainless mesh electrode geometry and size	57
Figure 26: Rubber stopper with electrodes and outlet T-junction attached.	58
Figure 27: Schematic of pressure vessel with electrical sub system. Pressure system color coded to blue. Electrical Sysytem color coded to red.	60
Figure 28: Diagram of flow system. Color coded to green.....	61
Figure 29: Current density over time during 20 minute intervals testing at 40 V	69
Figure 30: Current density averaged over all 20 minute intervals.....	70
Figure 31: Volumetric gas production rate for all intervals.	71
Figure 32: Average current density and average $\pm \sigma$ over time for 4 tests at 1000 psi	73
Figure 33: Average current density and average $\pm \sigma$ over time for 4 tests at 2000 psi	73
Figure 34: Average current density and average $\pm \sigma$ over time for 4 tests at 3000 psi	74

Figure 35: Average current density and average $\pm \sigma$ over time for 4 tests at 4000 psi	74
Figure 36: Average current density and average $\pm \sigma$ over time for 4 tests at 5000 psi	75
Figure 37: Average current density and average $\pm \sigma$ at each pressure	75
Figure 38: Average current density observed during testing at each voltage.....	77
Figure 39: Volumetric gas production at different voltages.	78
Figure 40: Effect of KOH concentration on current observed from 1-5 V.....	80
Figure 41: Effect of KOH concentration on current observed from 1.25-2.25 V.....	81
Figure 42: Cell Voltage For Electrolysis	82
Figure 43: Gas production at different voltages and KOH concentrations	83
Figure 44: Efficiency of electrolysis vs. voltages at selected KOH concentration.....	84
Figure 45: Effect of pressure change on electrolysis current density.....	86
Figure 46: Effect of pressure change on electrolysis current density.....	87
Figure 47: Effect of pressure change on gas production.....	88
Figure 48: Effect of pressure change on gas production.....	89
Figure 49: Effect of pressure change on system efficiency	91
Figure 50: Effect of pressure change on system efficiency	92

Nomenclature

u_m	Energy density by mass	MJ/kg
u_v	Energy density by volume.....	MJ/L
ΔH	Total enthalpy.....	W
h	Convective heat transfer coefficient	W/(m ² ·K)
\dot{m}	Mass flow rate	kg/s
σ	Standard deviation.....	
ϕ	Void fraction.....	m ² /m ²

Acronyms

FCV	Hydrogen Fuel Cell Vehicle
BPV	Electric Battery Powered Vehicles
LNG	Liquid Natural Gas Vehicles
CNG	Compressed Natural Gas Vehicles
BDV	Biodiesel or Biomass Vehicles
E85	Ethanol Mix Vehicles
GGE	Gasoline Gallon Equivalent
DOE	Department of Energy
NREL	National Renewable Energy Laboratory
EERE	Office of Energy Efficiency and Renewable Energy

UHP	Ultra High Pressure \geq 5000 psi
GC	Gas Chromatograph
LHV	Lower Heating Value
HHV	Higher Heating Value
PEM	Proton exchange membrane
SOEC	Solid Oxide Electrolysis Cell
AEC	Alkaline Electrolysis Cell
MEA	Membrane Electrode Assembly
SPE	Solid Polymer Electrolyte
PROX	Preferential Oxidation
JHE	International Journal of Hydrogen Energy
HiP	High Pressure Equipment Company
PSI	Pounds per Square Inch
ANSI	American National Standards Institute
PV	Photovoltaic
KOH	Potassium Hydroxide (Caustic Potash)
TSEL	Duke's Thermodynamics and Sustainable Energy Laboratory

Acknowledgements

Professors

Dr. Nico Hotz

Dr. Neal Simmons

Dr. Adrian Bejan

Dr. Heileen Hsu-Kim

Technical Advisors

Patrick McGuire

Steve Earp

1 Background

1.1 Current Affairs

It is estimated that our nonrenewable sources of liquid fossil fuels will last approximately 35 years from the time of writing this paper. These numbers are generated with relative accuracy using economic modeling of the world energy market and estimates of all remaining sources of liquid fossil fuels. These sources include all known accessible reserves, and predicted access to currently un-reachable reserves based on predicted technological advances (Shafiee and Topal 2009). For many, this means that gasoline driven vehicles will be replaced by a new technology within their lifetime. Beyond a certain lack of fuel there are also concerns regarding the uncertain environmental consequences of using these fuels. It is widely accepted that global climate change has been affected by the use of hydrocarbons which became prominent during industrialization in the 1800's. In the 200 years since then we have used approximately half of the known accessible fossil fuels and the temperature anomaly has grown to more than 0.5 degree Celsius (NOAA 2010). While it is hotly debated how much the temperature would need to rise to significantly affect the global climate, a large scale global climate change event could occur with anywhere from a 1-3 degree Celsius change. If this path continues the Intergovernmental Panel on Climate Change has cautioned that "the range of published evidence indicates that the net damage costs

of global climate change are likely to be significant and increase over time“, as described in Fig. 1(IPCC 2007).

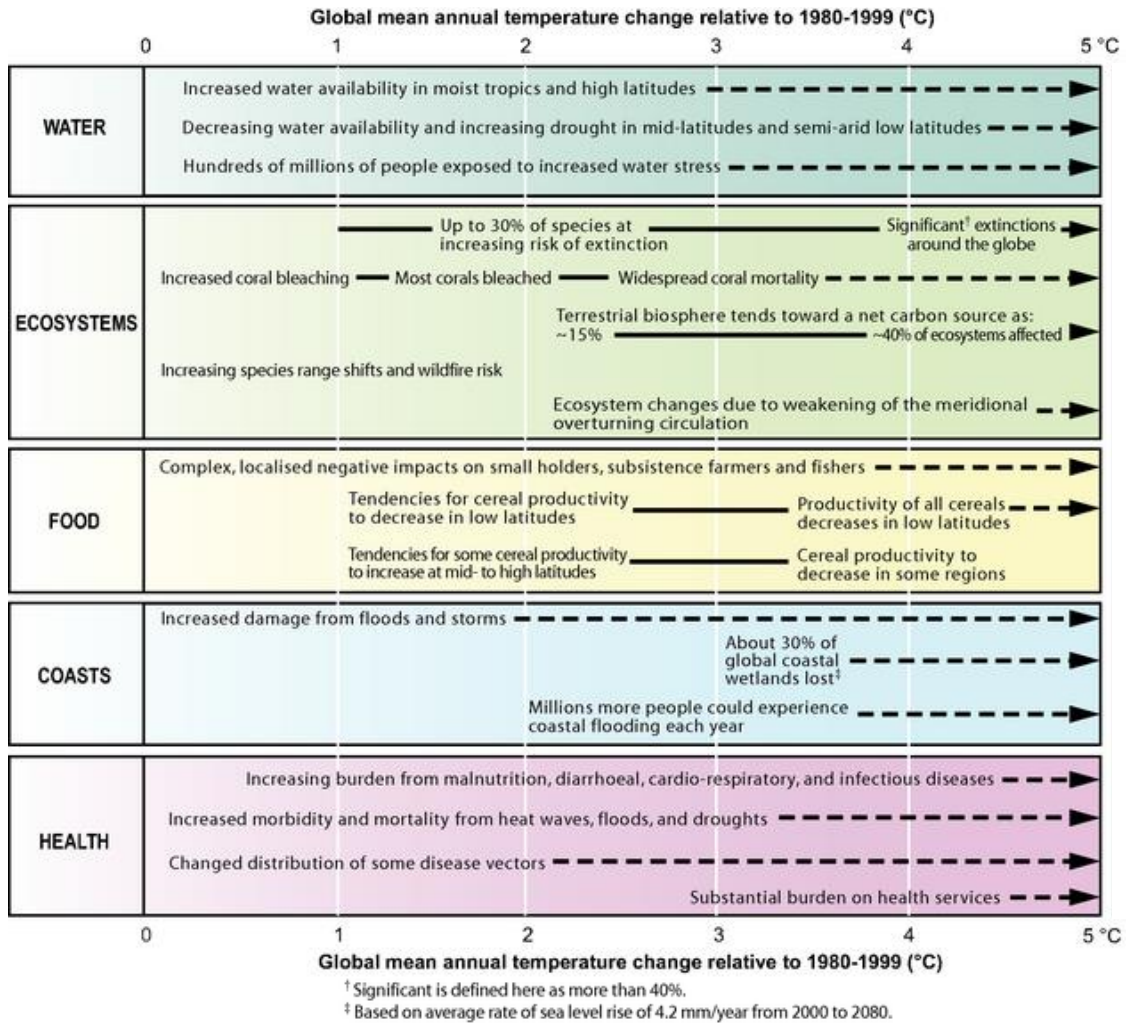


Figure 1: Impacts predicted to occur due to global climate change in five sections based on temperature increase. Affects will begin at temperature where the left of text is placed. Arrows indicate continued worsening conditions (IPCC 2007).

1.2 Alternative Fuels

As the scarcity, price, and environmental toll of fossil fuels continues to rise, scientists, governments, and fortune five hundred companies everywhere seek alternatives to these fuels. Several alternative fuels are currently vying to take over the immense roll gasoline plays as a fuel in transportation. Some of the most prominent of these fuels are Hydrogen, Electricity, Natural Gas, and Biomass. The vehicles which correspond to these fuels are, Hydrogen Fuel Cell Vehicles (FCV), Electric Battery Powered Vehicles (BPV), Natural Gas Vehicles (LNG/CNG), and Ethanol or Biodiesel Biomass Vehicles (E85/BDV). Biomass vehicles are domestically sustainable and can be integrated with current infrastructure and even current vehicles. However they compete with food crops for arable land and often the carbon cost of farming and processing them mitigates their environmental benefits. Natural gas vehicles are less polluting than gas and diesel vehicles but still rely on a non-renewable resource. Battery powered vehicles have significant promise as the most efficient use of electrical energy by direct storage and use in battery banks. The pitfall of BPV's is in the expensive, corrosive, and sometimes toxic materials used in batteries which have a limited lifespan before recharging becomes ineffective. An even bigger concern is the limited range of BPVs due to finite volumetric energy density of batteries. Since batteries cannot be recharged in a reasonable amount of time this makes long continuous trips almost impossible. The only solution to this problem besides a massive breakthrough in battery technology is the

standardization of a removable battery pack in cars so that a discharged pack could be swapped out for a charged one at a “fueling station”. This would mean a highly standardized and coordinated battery production and exchange program in which the refueling stations would have to monitor and replace outdated banks accounting for this cost in some way. It would also mean all BPV manufacturers getting on board with the same battery size, shape, placement, mounting scheme, connection devices and the same battery chemistry. Since current BPVs use the battery stack as a core component of the cars frame adding weight and rigidity to the design this seems unlikely. Not to mention the batteries themselves are typically as proprietary as an engine, so manufacturers are unlikely to share the same ones. This makes a standardized pack, fueling station, and connection device highly unlikely. Fuel cell vehicles which run off hydrogen gas are certainly the most environmentally friendly of all the current alternative fuel options. In fact when hydrogen is produced using electricity from renewable resources the only exhaust from an FCV is water vapor. However there is a loss of energy associated with the processes of converting electrical energy to hydrogen and then back again. This means the total energy efficiency from creation at the renewable source to use in a FCV is lower than a BPV. No process of energy conversion is truly reversible or 100% efficient so losses are incurred at each step between production of electricity and produced motive forces. Figure 2 from (Bossel 2006) shows the steps necessary to transform electrical energy into motion using two vehicle models. Note that each step has its own

average efficiency and that FCVs have more steps and therefore require more energy to run than BPVs. While it would seem from this graphic that FCVs are wasteful in comparison to BPVs there are many advantages to FCVs which BPVs cannot provide.

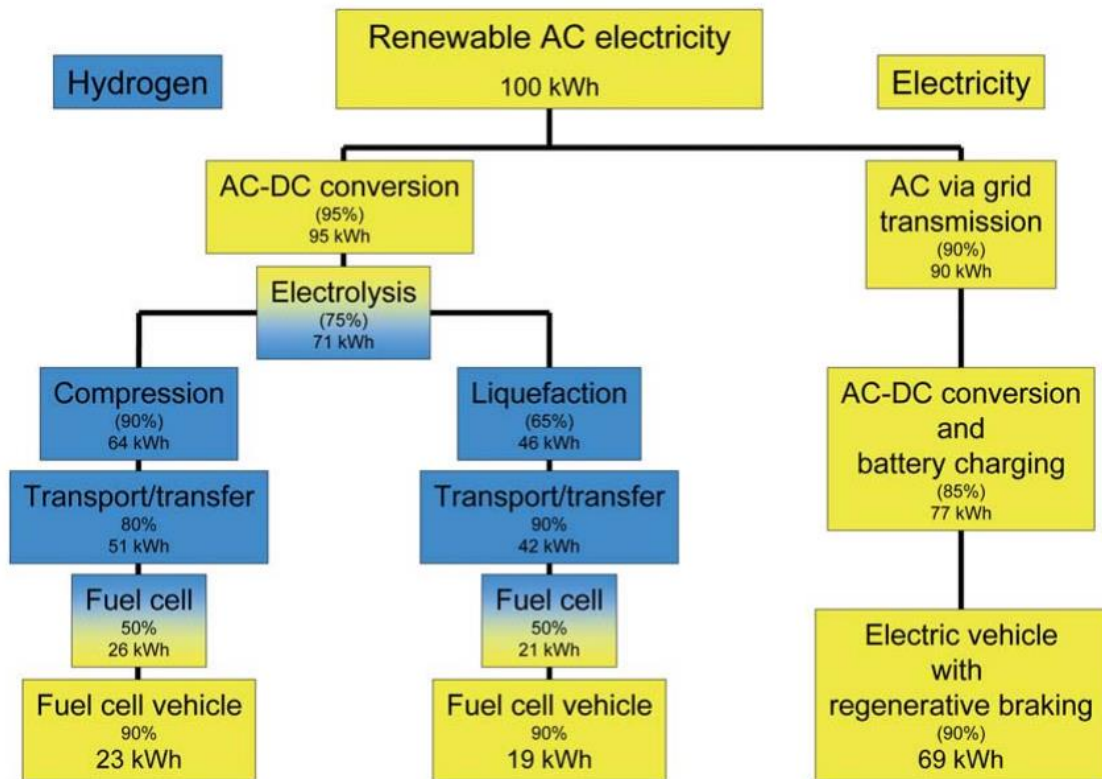


Figure 2: Electrical efficiency source to end use of BPV and FCV (Bossel 2006)

The primary benefit of using hydrogen as a fuel in transportation vehicles is that with increased pressure its volumetric energy density can exceed the limit of a battery significantly. This means that an FCV can have a longer range based on the pressure of its hydrogen tank with the same size allotted for either a battery or a tank. Another important benefit of using a pressurized hydrogen tank is that it can be refueled in a timely manner. This would allow for a similar experience to the one drivers currently

have of filling a tank quickly after a long travel distance. This is a major convenience which electric cars simply cannot offer because even the most advanced charging methods take hours to recharge the battery pack in a BPV.

The main barrier to implementation of any of these suggested alternative fuels is simply economic pressure based on cheap sources of liquid fossil fuels. The person or more likely multinational conglomerate of persons who can successfully tip the economic scale in favor of alternative fuels will likely be heralded as the father the 21st century economy. By design and by reduced use of hydrocarbons this new economy will promote more environmentally friendly practices.

1.3 Hydrogen Economy

The hydrogen economy would be similar to the current global economy in many ways. Since its inception many papers and even whole books have detailed the benefits and shortcomings of a hydrogen economy (Norbeck, Heffel et al. 1996, Ball and Wietschel 2009, Abbott 2010, Armaroli and Balzani 2011). Its electrical energy requirements would still be met using coal, nuclear, and renewable energy sources to generate electricity for the grid. The main difference between our current economy and the new hydrogen economy would be the distinct lack of liquid fossil fuels, namely gasoline and diesel. These fuels along with our fleet of transportation vehicles which run on them would be phased out in favor of FCVs, which run on hydrogen gas. In the ideal case, a larger portion of our electrical load requirements are met using renewable

resource generated electricity. The produced electrical load will fluctuate significantly based on the variable output of most renewable energy sources. This varying load is balanced by advanced electrolyzers which generate and store hydrogen for use as a transportation fuel during off peak hours. By running the electrolyzers mostly during off peak hours we can balance loads across the grid using electricity as cheaply and efficiently as possible. Since it is cheapest and easiest for power plants to produce constant load, storage of electrical power in other media will actually benefit the grid and reduce the cost of electricity. The added renewable loads which are variable can be stored via batteries for short term use and hydrogen for transportation and long term use. Storing hydrogen is more efficient over long periods because over time a battery will discharge regardless of use. Newly developed carbon composite tanks filled with hydrogen will last indefinitely without loss of energy. If hydrogen production can be decentralized, the overall efficiency of a hydrogen system is improved by lowering losses associated with delivery and transport of the fuel itself. This is a major contrast to our current system, in which our fuel is sourced from across oceans and continents. Another major benefit of decentralization is the reduction of middle man fueling stations and costs associated with up fits for these stations. Figure 3 depicts one example of how energy could flow in a hydrogen based economy. Note that fossil fuels are not omitted as they will still have a significant role in electricity and heat production but a reduced role in transportation. A study by NREL (Milbrandt and Mann 2007) showed that every

state in America could use renewable resources to produce hydrogen. Furthermore it showed that hydrogen produced by electricity from renewable resources in each state would be more than enough to replace gasoline as a transportation fuel.



Figure 3: A flow chart depicting a hydrogen based economy with integrated renewable and conventional electricity generation (Ball and Wietschel 2009).

2 Introduction to Hydrogen

2.1 Hydrogen as an energy carrier

Hydrogen as an energy carrier has a lot to offer and could be the future fuel of choice for transportation vehicles. Hydrogen has several main advantages over other competing energy carriers and could likely be used with great success in place of gasoline and diesel. Figure 4 shows both the volumetric and mass-specific energy density of many currently available energy carriers. It is important to note that hydrogen has the highest energy density per mass u_m in (MJ/kg) of all the energy carriers, both conventional and modern. Despite this, the figure also shows that hydrogen has a low volumetric energy density u_v (MJ/L) due to its gaseous form.

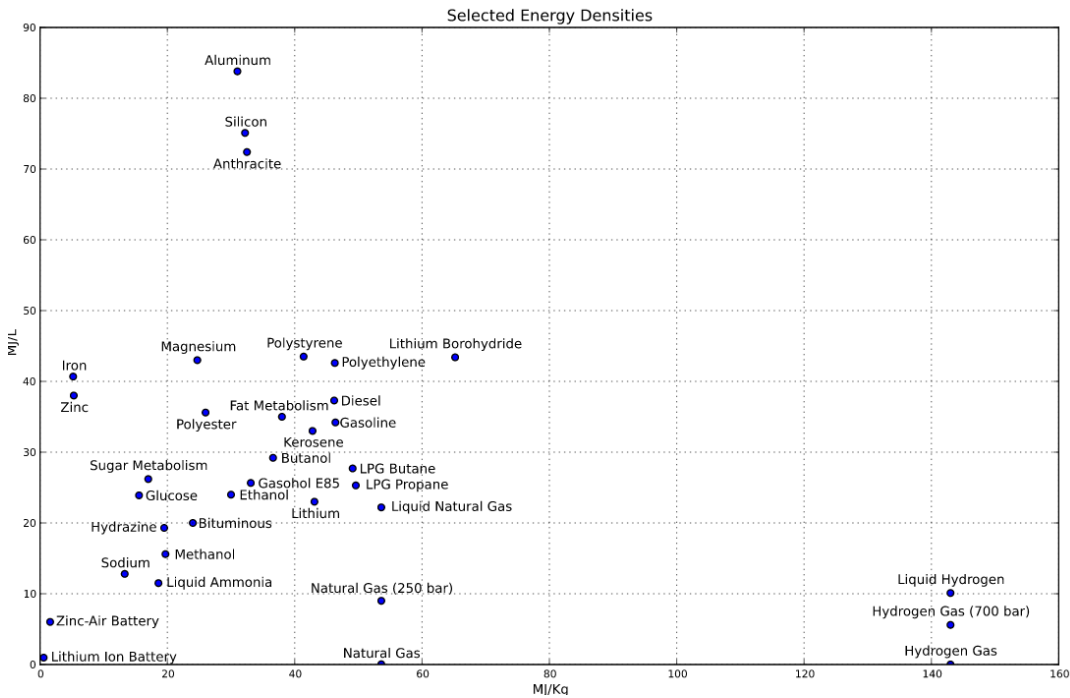


Figure 4: Energy carrier densities. Hydrogen is seen far to the right. Energy densities vary in accuracy due to HHV and LHV discrepancies and pressurization.

Volumetric energy density is important, as it determines the space needed to carry the fuel in mobile applications. Gasoline, for example, has moderate volumetric and mass-specific energy densities, explaining its ubiquitous use as a transportation fuel. One gallon of gasoline (3.785 liters), with a u_v of 32.35 MJ/L, contains 122.48 MJ of energy (GREET 2010). In comparison, hydrogen at atmospheric pressure has a u_v of 1.005e-5 MJ/L. A gallon of hydrogen then contains 3.804e-5 MJ, about 3.22e6 times less than gasoline. However, pressurized hydrogen can greatly reduce this disparity. The Department of Energy has set forth several pressure standards for hydrogen, ranging from 25 MPa (3.6 kpsi) to 70 MPa (10 kpsi) (Energy 2011). Hydrogen pressurized to 35 MPa (5 kpsi), also known as H35, is considered a baseline pressure for transportation purposes. At this pressure, the energy density rises to 2.7 MJ/L, making a gallon of gasoline contain only 11.9 times more energy.

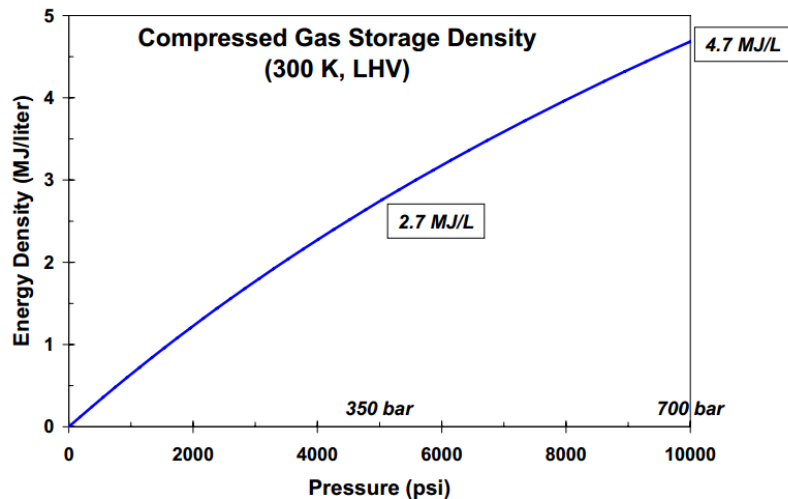


Figure 5: Compressed hydrogen gas energy storage density u_v vs. pressure source (Thomas and Keller 2003)

Figure 5 shows the increase in energy density of hydrogen gas with changing pressure up to 10_kpsi. Hydrogen at 10_kpsi known as H70 has an energy density of 4.7 MJ/L and is only 6.8 times less dense than gasoline. This is currently the top pressure target of the DOE for transportation vehicles. The pressure of hydrogen gas can be increased and the temperature lowered until the hydrogen turns into a liquid. At this point the u_v is 8.5 MJ/L. However, tanks for liquid hydrogen require cryogenic cooling, making them somewhat impractical for transportation. Without liquefaction hydrogen must undergo compression before it can compete as an energy carrier with conventional fuels. Pressurizing gases can be difficult due to their high compressibility and volatility. In most cases the process of compressing hydrogen is done after the hydrogen is generated, decreasing the overall efficiency of conversion. It is theoretically possible to avoid these losses by pressurizing liquid water before splitting it into hydrogen and oxygen (Appleby, Crepy et al. 1978, Leroy, Bowden et al. 1980, Onda, Kyakuno et al. 2004, Laoun 2007). Several thermodynamic factors suggest water electrolysis at high pressure and direct harvest of product gases is more efficient than electrolysis at low pressure and subsequent compression of the product gases. However the largest benefit of hydrogen when compared to other modern alternative fuels is its hydrologic cycle, which has no byproducts or harmful waste. This makes it a very attractive clean fuel when uncertainties about how environmental impacts might affect our future are considered.

2.2 Current hydrogen interest

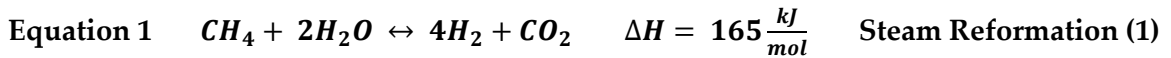
The U.S. Department of Energy (DOE) and National Renewable Energy Lab (NREL) recognize hydrogen as a potential hydrocarbon replacement and assemble a yearly progress report on current hydrogen research (Energy 2011). Several major journals including The International Journal of Hydrogen Energy (JHE), Journal of Power Sources, Catalysis Today, Journal of Electrochemistry, and many others also track advances. The aim of the JHE is stated as “To provide a central vehicle for the exchange and dissemination of new ideas, technology developments and research results in the field of Hydrogen Energy”. Hydrogen production also has potential to serve as an important backup fuel in several military installations. The US Navy determined that power from nuclear plants onboard aircraft carriers could be used to electrolyze seawater (Willauer 2010). Hydrogen produced in this way could serve as back up jet fuel for aircraft when traditional jet fuel was not available or its cost exceed \$6 per gallon gasoline equivalent (GGE). Similarly electrolyzers in submarines provide oxygen for inhabitants and hydrogen could be stored instead of diesel as a backup fuel for operations. In 2007 a DOE/NREL partner project with Giner Electrochemical Systems produced a 2000 psi Polymer Electrolyte Membrane (PEM) electrolyzer capable of producing hydrogen at ~4.5\$ per kg (Cropley and Norman 2008, Hamdan and Norman 2013). Interest in hydrogen energy is not isolated to government and academics either. Industry leaders like Toyota and General Motors have spent millions in research and

development of hydrogen as a fuel source for transportation. Since 2008 GM has been developing a solar powered high pressure electrolyzer for decentralized hydrogen production. The project successfully produced a 2000 psi solar powered electrolyzer with a total system efficiency from panel to movement in an FCV of 14% (Kelly, Gibson et al. 2008, Kelly, Gibson et al. 2011). Meanwhile this past month Toyota, the largest car manufacturer in the world, released all 5,680 of its patents regarding hydrogen powered fuel cell vehicles. Their effort to promote the development of the hydrogen vehicle is apparent by their statement at the time of release by VP Bob Carter, "The first generation hydrogen fuel cell vehicles, launched between 2015 and 2020, will be critical, requiring a concerted effort and unconventional collaboration between automakers, government regulators, academia and energy providers. By eliminating traditional corporate boundaries, we can speed the development of new technologies and move into the future of mobility more quickly, effectively and economically" (Toyota 2015). Interest is not contained to the automotive world however and with increased stress on an aging electrical grid people look to hydrogen as a possible stopgap. New renewable energy generation plants are typically geographically located and time dependent but not demand driven. Hydrogen generation and storage is a viable way to store energy produced for which there is no current load. With this vested global interest in mind we strive to create novel and efficient hydrogen technology which could supply future transportation and energy needs.

3 Electrolysis Methods And Theory In Literature

3.1 Hydrogen Production By Electrolysis

While there are many ways to produce hydrogen such as steam reforming a process which is used to produce the vast majority of hydrogen used today, electrolysis is the cleanest production method. This is mainly because processes such as steam reforming use heat and catalysis to split hydrocarbons or biomass. This produces hydrogen gas, but also leaves behind harmful by product gases such as carbon monoxide and dioxide. An example of this is given in equations 1, 2, and 3 which describe typical reactions that take place during the steam reformation of Methane.



Water electrolysis is the production of hydrogen and oxygen gas at purity as high as 99.9% by disassociation of the water molecule. By applying the electrical potential needed to break the chemical bonds we can cause this dissociation by eq. 4.



Since the electrolysis reaction produces only clean usable oxygen as a byproduct, electrolysis with electricity sourced from renewables is a much cleaner method of hydrogen production. There are currently five major types of electrolysis which are of

interest to both researchers and industry. Each has its own unique traits but all share the same reaction from Eq. 4 as their basis.

3.1.1 Microbial Electrolysis

Microbial electrolysis cells are similar to traditional electrolysis cells but exoelectrogen microbes are integrated in the electrodes as seen in Fig. 9. These microbes decompose organic material and produce electrons supplying some of the voltage required for water splitting. Since these microbes both lower the input power requirements of the system and help catalyze the reaction they can increase a regular cell's efficiency by 15% or more. Before these systems become commercially available, however, issues with methane production as a byproduct, feedstock selection, CO₂ emission and the impurity tolerance of the microbes will need to be addressed (Logan, Call et al. 2008)

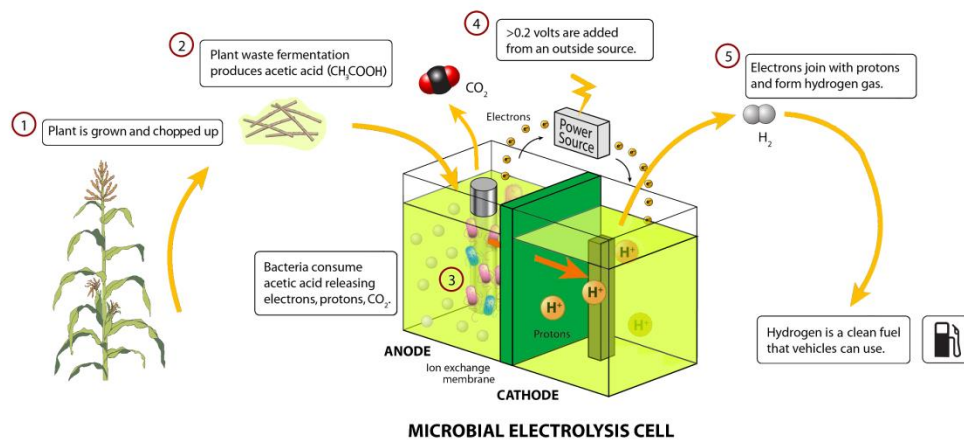


Figure 6: Microbial Electrolysis Cell courtesy of NSF (Deretsky 2012)

3.1.2 Photovoltaic Electrolysis

The most recent and hence least studied of the four processes is direct photovoltaic electrolysis. This process is simple and involves a p/n junction cell connected to water electrolysis electrodes directly. Ordinarily a PV cell would have a connected circuit where electricity would travel to a selected load or battery. In this case the circuit is completed by direct connection to the electrolysis reaction, as shown below.

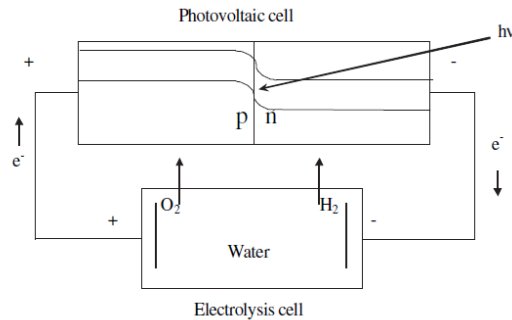


Figure 7: Diagram of a photovoltaic electrolysis cell (Zeng and Zhang 2010).

Progress in photoelectrical cell research has been hindered by the inability to find a robust semiconductor material with a bandgap matching the electrolysis reaction (Khaselev and Turner 1998). This is important because if the electrochemical reaction energy requirements are not matched to that of the semiconductor PV cell, surface oxidation of the cell will occur. Current devices with electrodes which are durable in the aqueous electrolysis environment have efficiencies of approximately 5% (Zeng and Zhang 2010). Until further development in stable semiconductor materials is made these devices cannot compete with existing technology.

3.1.3 Solid Oxide Electrolysis

Solid oxide electrolysis also known as steam electrolysis is another process currently being considered for large scale hydrogen production. In a solid oxide electrolysis cell (SOEC) high temperature steam is fed to the cathode side of a cell which is separated by an electroceramic solid electrolyte, generally yttria stabilized zirconia (Brisse, Schefold et al. 2008).

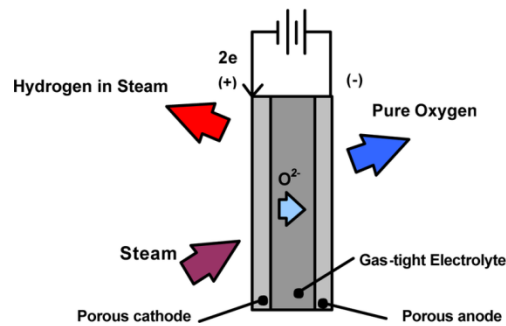


Figure 8: Solid Oxide Electrolysis Cell Source (Energy 2011)

The steam temperatures necessary for efficient operation are in excess of 1000 °K but supply part of the energy needed for electrolysis thermally lowering the electrical requirements by up to 35%. However the energy needed to heat the steam outweighs this benefit making SOEC's less efficient than some other technologies. The benefit of SOEC's comes in the construction of the solid oxide cell which unlike liquid electrolytes or polymer membranes is not sensitive to flow distribution issues and can catalyze carbon dioxide/monoxide shifts (Tao and Virkar 2006). Challenges for improving SOEC's include preventing coke build up, improving durability/temperature resistance of the solid electrolyte, and improving efficiency possibly through use of waste heat.

3.1.4 Polymer Electrolyte Membrane Electrolysis

Polymer electrolyte membrane (PEM) electrolyzers are among the most studied and best developed of hydrogen production systems. Their high efficiency and ability to operate at high current density makes them the chief competitor with traditional alkaline cells. A typical diagram of a PEM electrolyzer is shown in Fig. 12 below. PEM cells are excellent at minimizing gas crossover and have superb conductivity but their high capital and maintenance costs sometimes make them uneconomical. The membrane electrode assembly (MEA) of a PEM cell typically contains expensive noble metals and the Solid Polymer Electrolytes (SPEs) are not cheap or particularly robust.

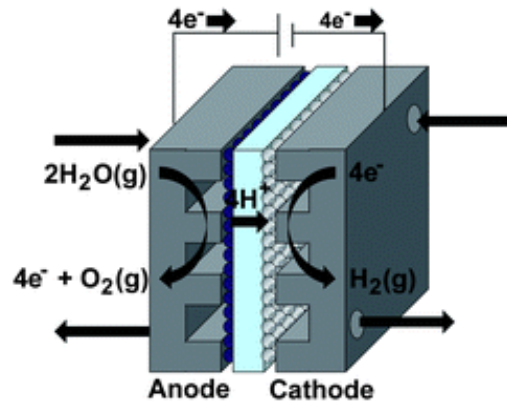


Figure 9: Polymer Electrolyte Membrane cell (Spurgeon and Lewis 2011)

High pressure PEM cells hold promise in the future of electrolysis but even a slight differential pressure across the SPE can cause it to tear.(Spurgeon and Lewis 2011).

To bolster the membranes ability to handle pressure variation developers of high pressure PEM cells have created complex porous laser micro-machined polyimide support architectures(Marangio, Santarelli et al. 2009). A PEM electrolyzer funded by

the DOE and developed by Giner Electrochemical systems was capable of hydrogen production at pressures up to 5000 psi. However the capital and maintenance costs associated with the complex supported membranes were not sustainable so the electrolyzer was redesigned to function at 2000psi (Cropley and Norman 2008).

3.1.5 Alkaline Electrolysis

Alkaline electrolysis is a mature industrialized process for producing clean hydrogen from electricity in an aqueous electrolyte solution. The efficiency of this process in commercial units is approximately 60% about 10% less than PEM cells. It accounts for 4% of the total hydrogen produced annually.

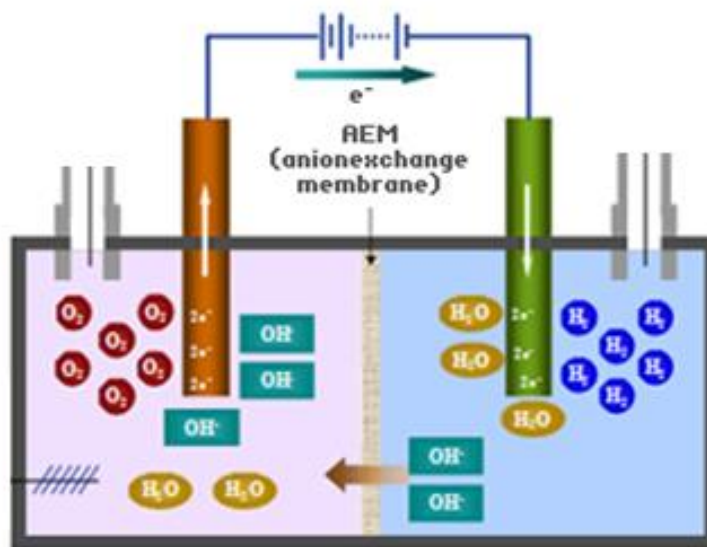


Figure 10: Alkaline Electrolysis Cell. Note that there is no need for a membrane in this type of cell but it can be added for increased gas purity.

Currently 95% of the hydrogen manufactured comes from the reformation of fossil fuels (EERE 2014). Figure 13 shows a typical alkaline electrolysis cell (AEC) which consists of two electrodes, a microporous membrane, and an electrolyte solution. Alkaline cells have the advantage over other electrolysis cells of being a simple and mature technology. Originally developed in the 1920's hydrogen production by alkaline electrolysis was commercialized for use in ammonia production and crude oil reforming. In order to use AECs for hydrogen generation effectively we must improve their electrical efficiency. This is because the majority of the cost associated with hydrogen electrolysis comes from the electricity needed to drive the reaction. Challenges to improve AECs include improving conductivity and developing electrodes which are more active but still durable. Stainless steel and Nickel alloys have been proven as active electrode materials with high corrosion resistance and economic availability (Zhang, Lin et al. 2010). Optimization of the geometric parameters including gap spacing, electrode shape/size, recirculation, and bubble formation can significantly affect process efficiency (Nagai, Takeuchi et al. 2003) (Zhang, Merrill et al. 2010). High and ultra-high pressure alkaline electrolysis can produce hydrogen gas that is already at pressure with less difficulty than PEM systems. In some cases production at ultrahigh pressure can negate entirely the need for a secondary gas compressor and drying systems (Hamdan 2008, Hamdan and Norman 2013) This process increases the overall efficiency by eliminating post production pressurization and drying energy and maintenance costs.

3.1.6 Summary of State of the Art Technologies

A collection of these state of the art technologies, their approximate efficiency, and commercial feasibility is compiled for review in Table 1. This table shows the estimated term in which the current state of the art technology could be used for hydrogen production. Note that not all processes can be scaled economically for large output operation but could still be used for decentralized production.

Process	Feedstock	Approximate Efficiency %	Availability
Steam Reforming	Hydrocarbons	75	Commercial
Partial Oxidation and Auto-thermal Reforming	Hydrocarbons	75	Commercial
Aqueous Phase Reforming	Carbohydrates	45	Medium Term
Biomass Gasification	Biomass	45	Commercial
Plasma Reforming	Hydrocarbons	10	Long Term
Organic Photolysis	Sunlight	0.5	Long Term
Thermochemical Water Splitting	Heat Chemicals	N/A	Long Term
Microbial Electrolysis	Biomass Electricity	75	Long Term
Photovoltaic Electrolysis	Sunlight	12	Long Term
Solid Oxide Electrolysis	Heat Electricity	50	Medium Term
Polymer Electrolyte Membrane Electrolysis	Electricity	65	Commercial
Alkaline Electrolysis	Electricity	55	Commercial

Table 1: Various technologies and their current state

3.2 Electrolysis Theory

3.2.1 Thermodynamics

A simple view of alkaline electrolysis as well as the basic equation for electrolysis or water splitting is given in figure 10 and equation 4. Information on enthalpy of formation and entropy can be found for the hydrogen, oxygen, and liquid water species involved in properties tables (Moran and Shapiro 2008). By calculating the change in Gibbs energy we can determine the reversible potential of an electrolysis cell as 1.23V seen in equations 5, 6, 7, and 8.

$$\text{Equation 5} \quad \Delta S^\circ = S^\circ_{H_2} + \frac{1}{2}S^\circ_{O_2} - S^\circ_{H_2O} = 0.163 \frac{kJ}{molK} \quad (5)$$

$$\text{Equation 6} \quad \Delta H^\circ = H^\circ_{H_2} + \frac{1}{2}H^\circ_{O_2} - H^\circ_{H_2O} = 286.03 \frac{kJ}{mol} \quad (6)$$

$$\text{Equation 7} \quad \Delta G^\circ = \Delta H^\circ - T\Delta S^\circ = (286.03 - 0.163 * T) \frac{kJ}{mol} \quad (7)$$

$$\text{Equation 8} \quad V_{Rev} = \frac{\Delta G^\circ}{n * F} \quad n = \text{electrons} \quad F = \text{Faradays constant} \quad (8)$$

However this reaction is endothermic requiring an input of heat to operate adiabatically and so this reversible potential is less useful than its counter-part deemed the thermoneutral voltage. This voltage is described by equation 9 and simulates a reaction where no heat is transferred in or out of the system an ideal condition in which the cell operates near 100% efficiency. A thermoneutral cell would operate at 1.48V requiring no external source of heat but disregarding real life system losses caused by over potentials.

$$\text{Equation 9} \quad V_{Thn} = \frac{\Delta H^\circ}{n * F} \quad n = \text{electrons} \quad F = \text{Faradays constant} \quad (9)$$

Current literature has provided extensive theoretical calculation of these ideal cell voltages for a range of temperatures and pressures (Ulleberg 2003, Onda, Kyakuno et al. 2004, Laoun 2007, Todd, Schwager et al. 2014). Below in figure 11 a sample of these calculations obtained using thermodynamic analysis including virial coefficients for high pressure and temperature species.

p (MPa)	$E_{298,p}$ (V)	$E_{373,p}$ (V)	$E_{523,p}$ (V)
0.101325	1.229	1.167	(1.051)
10	1.317	1.278	1.207
22.064	1.332	1.297	1.234
40	1.343	1.311	1.255
70	1.354	1.325	1.275

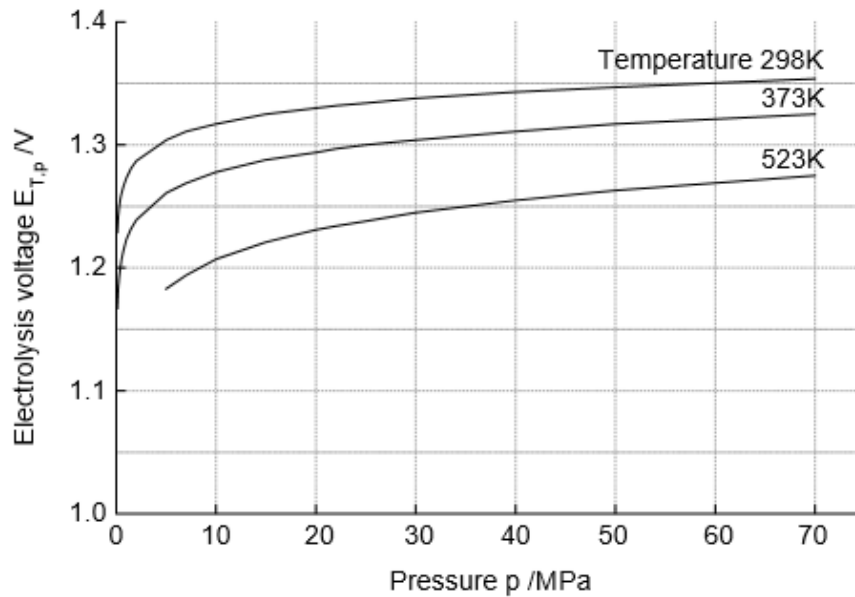


Figure 11: Predicted Reversible Electrolysis Voltage (Onda, Kyakuno et al. 2004)

Their predictions while valuable ignore completely real life system losses caused by over voltages and internal resistances. The authors of these papers openly admit to the

unrealistic nature of the results claiming the data for real life systems simply does not exist and therefore cannot be considered in their works.

3.2.2 Overvoltages and Efficiency

A more accurate representation of cell voltage is presented in figure 12 by including although not to precise scale the over voltages encountered in a real life system.

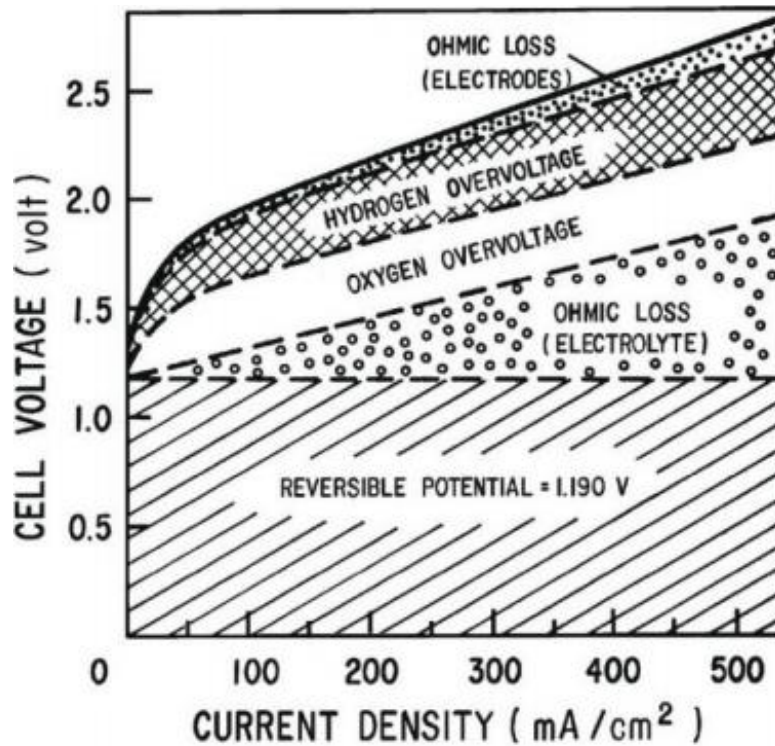


Figure 12: Distribution of electrolysis cell voltage (Ohata 2009)

Beyond the reversible potential there are 5 common over voltages which contribute to an increase in cell voltage and thereby a decrease in system efficiency. The first and also typically the smallest overvoltage is encountered at the electrodes. This is the ohmic loss

due to the resistance of the electrode itself and the circuitry which connects it to a power source. In a typical industrial alkaline cell electrodes are made of stainless steel and nickel or else titanium and steel alloys. While these are decent conductors they do have higher resistances than other metals such as platinum or copper. To understand why these materials are not used one only needs to consider the cost of platinum on a large scale or the corrosion of copper in the presence of electrolytes and high currents. The second over voltage encountered is hydrogen and oxygen evolution reaction. While they are presented as equals in figure 12 the more complicated oxygen evolution reaction often presents a slightly larger overvoltage. To reduce this loss you must consider the surface and micro scale geometry of the electrodes as well as the activity of the material selected. Electrode material and geometry is hotly debated and highly studied always with the goal of forming a highly active yet durable alloy which is cost effective for large scale systems. Finally we reach the largest overvoltage encountered in real life systems the ohmic loss through the electrolyte. To reduce this loss you must select a strong electrolyte such as those used in industry KOH and NaOH and apply it in a high concentration. You can also reduce the distance between the electrodes to lower this effect but only to a certain extent before bubble masking becomes an issue. The effect of reduced distance between the electrodes is shown by figure 13 to be effective even at low voltages where the ohmic loss is smaller.

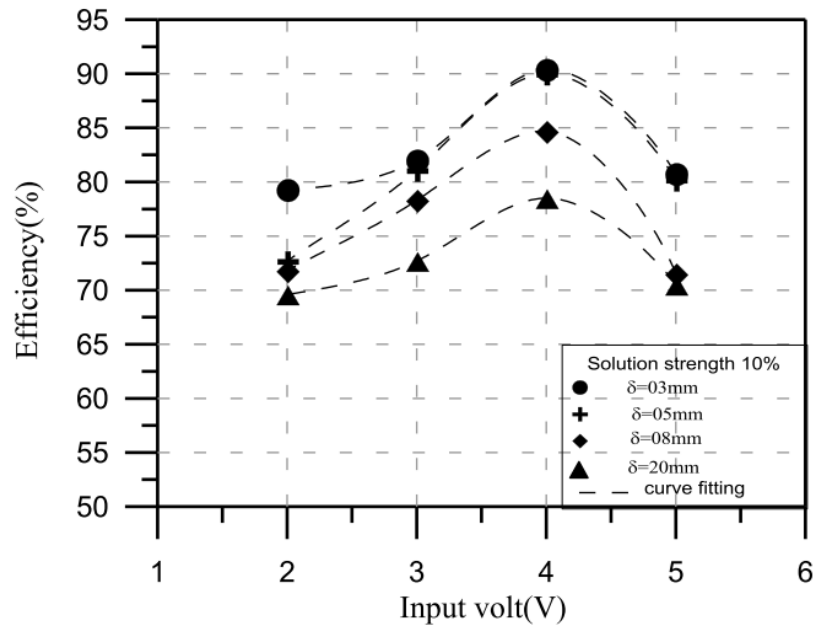


Figure 13: Effect of electrode spacing on electrolysis efficiency (A-F.M. Mahrous 2011)

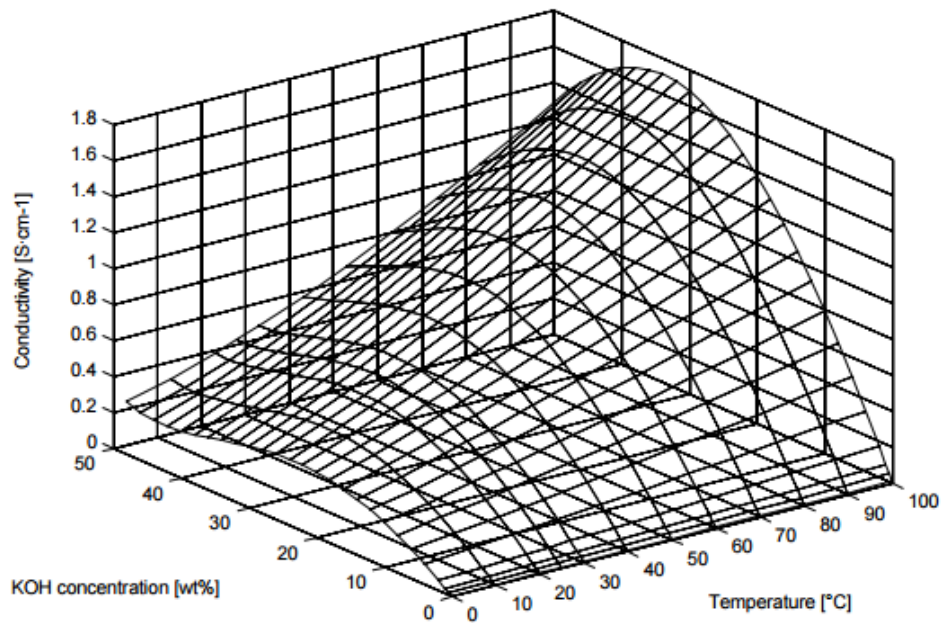


Figure 14: Conductivity of aqueous KOH vs concentration and temperature (R.J. Gilliam 2007, Frank Allebrod 2011)

From conductivity data such as that seen in figure 14 we might also select the best concentration of electrolyte based on conductivity. For KOH it is approximately 30% by weight however industry and scientific units typically use a range of concentrations between 20 and 40%. Use of lower concentrations may be due to the highly corrosive nature of strong electrolytes in an effort to increase durability of systems.

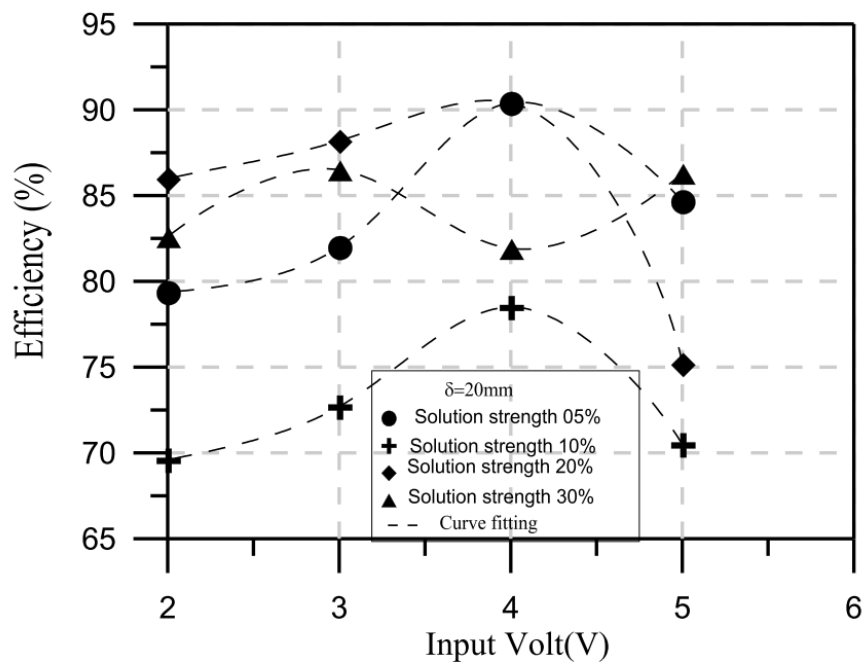


Figure 15: Effect of KOH concentration on electrolysis efficiency (Ohata 2009)

Real life low pressure data suggests that the efficiency of electrolysis based solely on concentration changes in the solution is less straightforward than simple conductivity as seen in figure 15. To further discuss efficiency of an electrolysis system we should define efficiency as it is reported in other works and as we report it in this work. Efficiency can be reported in two ways the first of which is how most theoretical works define

efficiency called the electrolysis efficiency. Electrolysis efficiency as shown in equation 10 is simply the ratio of the thermo-neutral voltage for electrolysis and the observed voltage of electrolysis in a real system. It is important to note that if a cell could operate at the theoretical reversible cell voltage with input of heat or significant loss this equation could result in efficiency greater than 100%.

Equation 10
$$\eta = V_{Thn}/V_{obs} \quad (10)$$

The second definition of efficiency is a more realistic isothermal system efficiency which uses the product gas as the output and electrical energy supplied as the input. The energy output from the system is calculated as the lower heating value of produced hydrogen gas. This is divided by the electrical energy input to the system by the power supply during electrolysis. The isothermal assumption applied to this calculation is largely accurate as long as the system does not show significant variance in temperature during operation.

Equation 11
$$\eta = \frac{(X_{mLH_2}) * 10.2 \frac{J}{mL}}{E_I} \quad X = \text{mL of Hydrogen} \quad E = \text{Electrical Energy} \quad (11)$$

Scientific alkaline electrolysis systems have reported efficiencies in excess of 86% but do not factor in reasonable rates of production. The need for a greater gas production rate is why typical industrial electrolyzers use a higher voltage even though it reduces the efficiency of electrolysis to as low as 40%. Since the main cost associated with alkaline electrolysis is that of the electricity input all efforts must be made to increase the efficiency of these cells if they are to be economically competitive with other technology.

One thought might be to increase the temperature at which the electrolysis takes place as this will reduce the cell voltage necessary for electrolysis. The effect of raising temperature is shown in figure 16 as a slight decrease in the electrical energy needed. Since electrical demand is the main cost in electrolysis this first seems quite favorable at first but then you must consider the added heat energy and its source as it is unlikely to be waste heat at such temperatures. Furthermore the total energy demand increases slightly with increased temperature and the physical and safety challenges of high temperature electrolysis in a real system are vast.

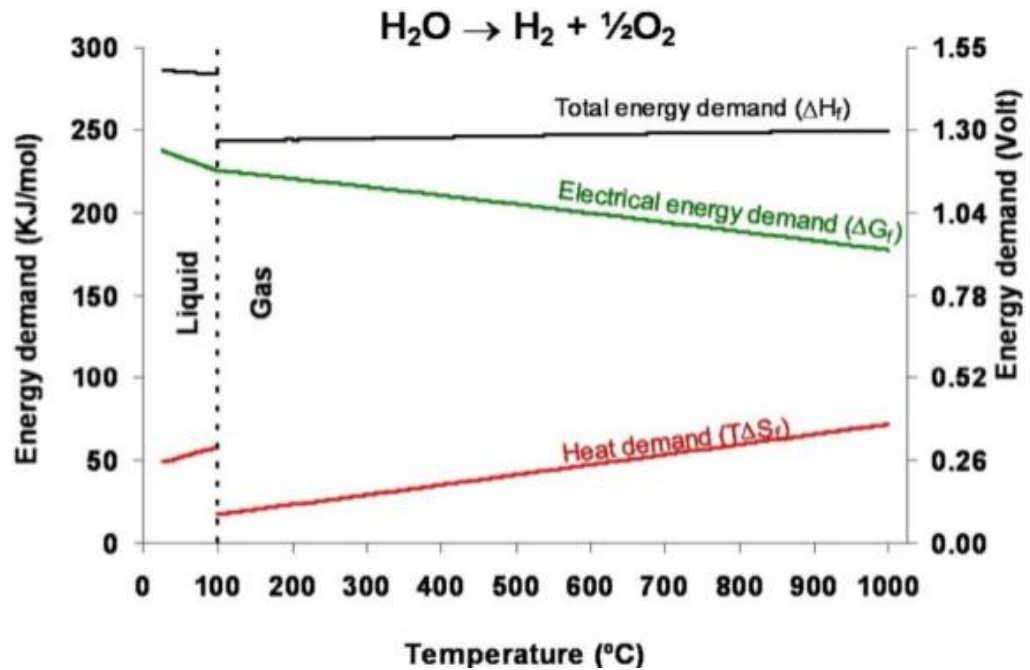


Figure 16: Energy demand of electrolysis vs temperature

3.2.3 Pressurization

To this point only theoretical works exist which predict what behaviors might occur in high pressure electrolysis systems. These works admit a lack of real system data to back their claims and fall short of describing how real life over voltages may or may not be affected by increases in pressure. Some experiments have been done in the low to medium range of pressure but a lack of data in the high and ultrahigh pressure range leaves the scientific community with little to bolster these ideal calculations. The main advantage of a high pressure electrolyzer is the ability to produce product gases which are already at the desired operating pressure. The product gas desired in this case is hydrogen at 5000 psi, the operating pressure for use in typical FCVs. Oxygen at 5000 psi will also be produced and is a saleable by product. In order to produce gas at this pressure a traditional electrolyzer would need to produce low pressure gas and then employ a compressor to pressurize its product gasses up to 5000 psi. The disparity between the work required to pressurize a liquid for the high pressure electrolyzer and the work required to pressurize the gas from a traditional one can be calculated. A simple analysis of the work needed to pressurize a liquid compared to the work required to isothermally pressurize an ideal gas mixture is shown in figure 17. The work required for compressing water was determined using values for compressed liquid enthalpy from known data tables. Work for compression of product gases is

determined using Eq. 12 which assumes an ideal gas mixture undergoing isothermal compression(Moran and Shapiro 2008).

Equation 12
$$W_{gas} = -\int_{V_0}^V p dV = -nRT * \int_{V_0}^V \frac{1}{V} dV = -nRT * \ln \frac{V}{V_0} \quad (12)$$

From figure 17 it is obvious that pressurizing a gas takes much more work than pressurizing a liquid at all pressures until the compressibility of the gas become minimal. At this pressure the properties of liquids and gases become similar and the work required for pressurization should become the same.

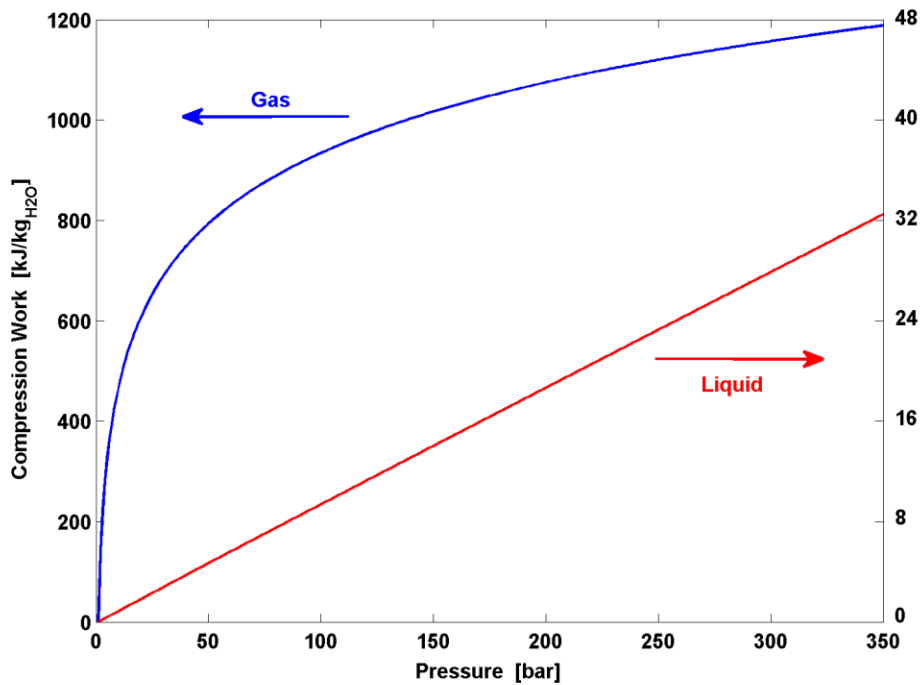


Figure 17: Work for compression of 1 kg liquid water compared to work for compression of gases generated from 1kg of water. **Note that the scale for liquid compression (right) is 25 times smaller than the scale for the gas compression (left).

The ratio between the work required for liquid and gas compression at sample pressures up to the goal pressure of 5000 psi can be seen in Table 2. This shows that liquid compression requires one to two orders of magnitude less work than compression of the corresponding gases at the pressure relevant for this work.

Pressure (psi)	1000	2000	3000	4000	5000
Work Ratio (W_{gas}/W_{liquid})	129.7	75.63	54.75	43.40	36.18

Table 2: Ratio of work needed to compress gas vs. liquid at sample pressures

More rigorous thermodynamic examinations of gains associated with these claims can be found in (Appleby, Crepy et al. 1978, Leroy, Bowden et al. 1980, Onda, Kyakuno et al. 2004, Laoun 2007, Ganley 2009, Todd, Schwager et al. 2014). These references use unique methods but all arrive at similar conclusions. They claim that high-pressure electrolysis systems should be significantly more efficient despite the increases in cell voltages that are predicted at high pressures.

4. Novelty

Currently only two examples of working ultra-high pressure (UHP) electrolyzers have been published. These UHP electrolyzers were both built by private companies: Avalence LLC and Giner Electrochemical Systems under DOE grants at costs of 2.41 and 2.27 million dollars respectively. Since their designs are proprietary, only limited information on these systems could be published or released leaving much to be desired in the area of UHP electrolyzer research. These systems were designed in a way that is cost prohibitive and inflexible with no ability to change and characterize the variable involved in high pressure electrolysis. In fact, the Giner PEM system was considered uneconomical at 5000 psi and further development of this system has been limited to 2000 psi (Hamdan 2008). A new DOE contract with Giner seeks to lower the cost of this high pressure PEM unit by developing a cheaper MEA but no further effort to increase the pressure is made (Hamdan and Norman 2013). Avalence LLC developed a 2500 PSI alkaline electrolysis system and proposed further development of a 6500 PSI system. However they lost their continued DOE funding because they were unable to produce their portion of the project's funding and have since suspended future research on ultra-high pressure electrolysis (Dunn and Maurterer 2011).

In order to study the proposed benefits of UHP electrolysis and characterize real life behavior of such a system we have developed a novel low cost UHP electrolysis system. This system is extremely economical costing approximately 20,000 dollars and

its simplicity allows it to be very flexible. With a working pressure of 5000 psi and at a cost approximately 100 times less than its commercial counterparts this system is the first of its kind. While it's overall efficiency may not rival the multi-million dollar units, the setup will allow for experimentation with many different electrode materials, sizes/shapes, catalysts, and electrolyte fluids in order to develop an optimum design for UHP electrolysis. The simplicity of the design allows for maximum flexibility in the electrolyzer cell with little to no modification of the pressure vessel, piping and flow, or pressure control system.

The goal of this experimental setup is to prove the theoretical gains of proposed UHP electrolysis and further current research regarding the behavior of such a system. Current cell design and catalyst material research exists primarily in analytical modeling or in low pressure environments (Chen and Lasia 1991, Fan, Piron et al. 1994, Nagai, Takeuchi et al. 2003, Crnkovic, Machado et al. 2004, Caspersen and Kirkegaard 2012, Marinha, Salvia et al. 2012). Using previous theoretical and related low pressure work we hope to characterize the behaviors of a high pressure system allowing for further optimization of electrolysis variables. Experimentation will also aim to prove the legitimacy of theoretical gains in a real life ultra high pressure apparatus.

5. Materials and Construction

5.1 Pressure Vessel System

The core component of high pressure hydrogen production is the pressurizing vessel or housing for the electrolysis cell. The vessel was designed to resist cyclic loads of pressurization, be resistant to numerous forms of corrosion, and ensure no water or gas leakage at pressures up to 5000 psi.

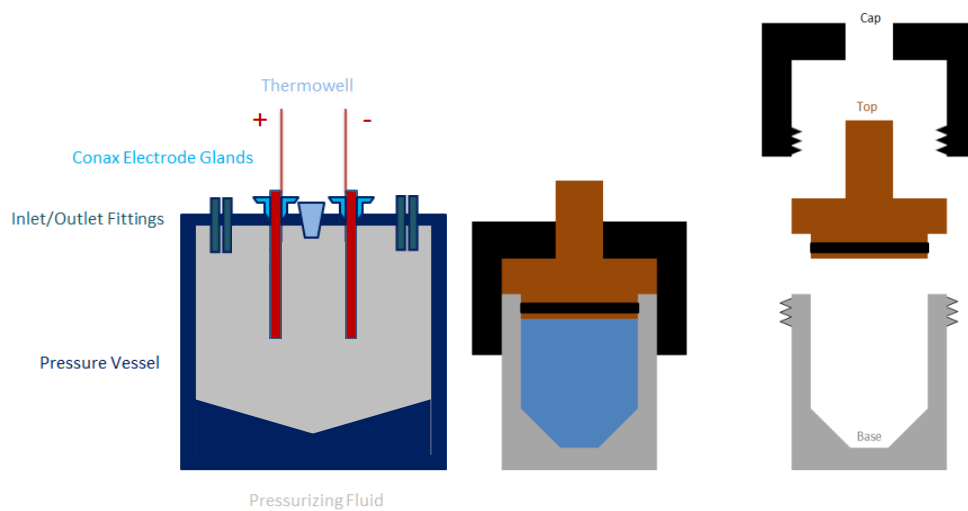


Figure 18: Simplified, two-dimensional construction of pressure vessel. Does not include electrolysis components

5.1.1 Vessel

316 stainless steel was selected as the vessel material for its excellent chemical compatibility, high corrosion resistance, and strength (Janssen 2004). Due to the machining requirements and potential safety hazards of the vessel, HiP, a high pressure equipment company was consulted for its production. Since safety was a top priority the fabricated vessel was ANSI certified before being delivered. Certification assured

safety and reliability with a working pressure of 5000 psi and a top pressure of 7500 psi. The vessel is cylindrical in shape, with a concentric interior that has a conical bottom taper. The vessel has a 5 inch inner diameter and approximately a 7 inch outer diameter and holds approximately 5 L. The top of the vessel is threaded on the exterior wall to accept the vessel cap. The weight of the cap and size of the threads plus the pressure which is applied when the vessel is in use dictates the use of a copper based lubricant to prevent seizure.



Figure 19: Pressure Vessel, Fabricated by HIP according to our design and rated by ANSI for a working pressure of 5000 psi.

5.1.2 Top

The top, like the base, is fabricated using 316 stainless steel to resist corrosion and cyclic high pressures. It has three concentric tiers, one for each function it was designed to perform. The first tier is five inches in diameter and seats itself inside the chamber. An external Nitrile Buna-N O-ring inside a groove in the top sits against the interior wall of the vessel sealing the system. The second tier, which sits on top of the vessel and is flush with its exterior, serves to increase the structural integrity. The third tier at approximately 3 inches in diameter provides a junction for the fittings attached to the vessel. These connections travel through the top into the vessel chamber and provide access during testing. The top and its tiers and main components are shown in Fig. 16

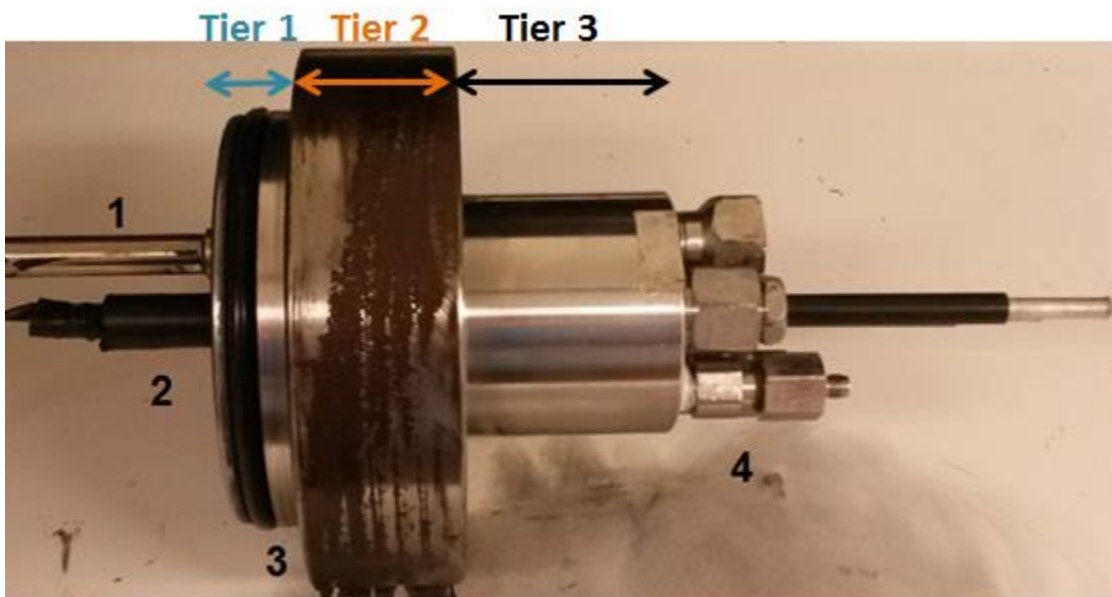


Figure 20: Vessel Top Side view; 1: Thermowell, 2: Insulated internal electrode, 3: Buna N O-ring in groove, 4: Inlets/Outlets

The top of the vessel was fabricated with five connections to the pressure vessel oriented in a circle around the top. The design provided to HiP had one hole for a thermowell, two for mass flow, and two for electrical supply.

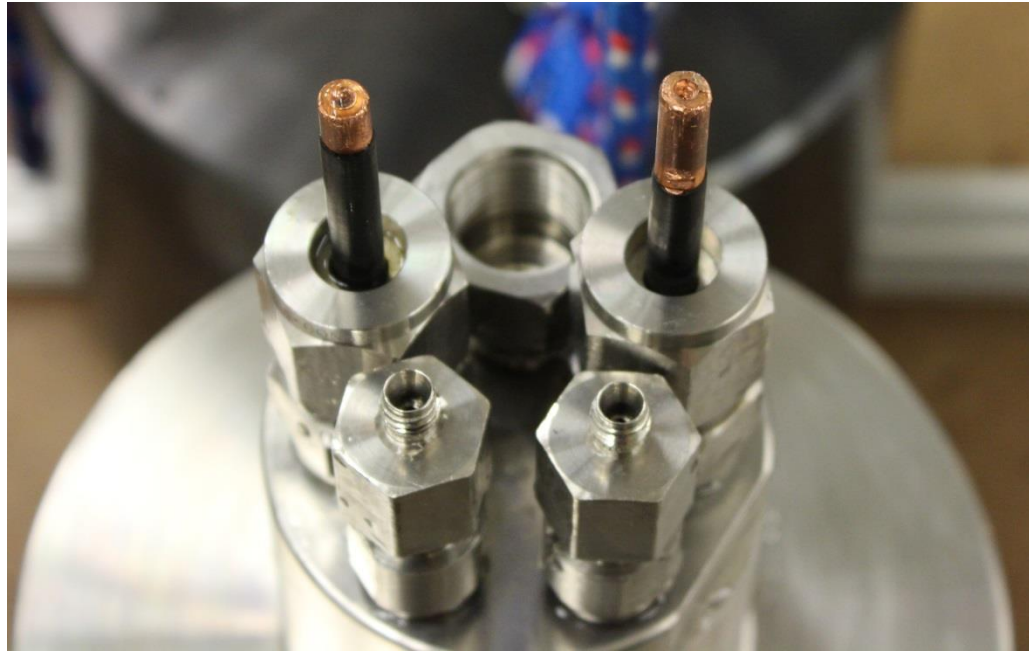


Figure 21: Overhead view of pressure vessel top. Clockwise from 12 o'clock: Thermowell, positive electrode, flow outlet, flow inlet, negative electrode.

5.1.2.1 Thermowell

In the top tier of the pressure vessel, a $\frac{3}{4}$ inch NPT hole was tapped for the 5 inch 445SS Omega Scientific thermowell. A thermowell was included in the design to monitor the temperature of the vessel during electrolysis. The temperature is important because it affects the thermodynamics of the reaction and because the system was rated by ANSI for safe operation below 100 degrees Fahrenheit. Higher temperatures could compromise the system and therefore must be measured to ensure system integrity and

safety. Accurate thermodynamic analysis of the reaction also requires monitoring and accounting for any change in temperature during testing.

5.1.2.2 Mass Flow

Special high-pressure fittings with a conical nozzle were used to ensure no leakage at the flow inlet and outlet connections to the system. However these fittings required the use of non-flexible external tubing and three piece fittings for each change of direction. Using this tubing would have been costly and was not practical for this application. Instead the design called for the use of $\frac{1}{8}$ inch outer diameter flexible 316 stainless steel tubing with Swagelok fittings. In order to facilitate the use of this modular, inexpensive, and repeatable design a fitting that transferred the ultra-high pressure conical fitting to the Swagelok fitting was designed and fabricated. Sound engineering practice was used to design this in-house part and computer simulations of the part were performed prior to its use to ensure it was safe at the required pressure.

5.1.2.3 Electric Fittings

Two electrodes are needed to perform electrolysis and these connections must be electrically insulated from the rest of the vessel. The stainless steel solid rod input electrodes were pressure fit into Deralin plastic tubing to insulate them from the fittings and thereby the rest of the pressure vessel. The fittings chosen to seal the solid rods were Conax PG4-275-A-L glands. The meaning of these numbers is, in order, bore size, diameter of tube, threaded cap style and "lava" proprietary composite ferrule. These

glands squeeze a conical crush ferrule made of proprietary material onto the electrode, ensuring no leaks and keeping them in place. The Conax fitting screws into the top of the vessel via 1/2 inch NPT threads. Figure 18 shows the cross section of a Conax gland and provides a depiction of how the PG4 glands operate.

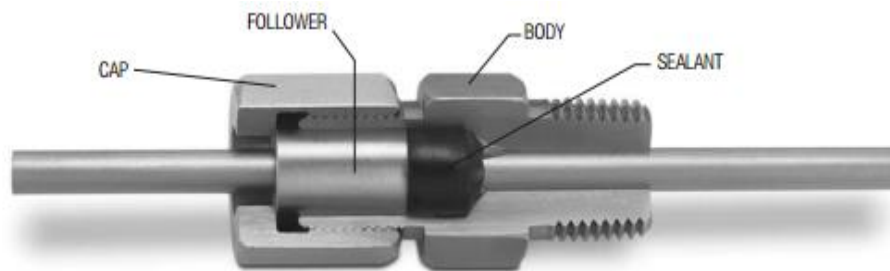


Figure 22: Technical drawing of a Conax gland for the electrode. Pressure rating from vacuum to 10,000 psi (Conax 2014).

5.1.3 Cap

To ensure the top stayed seated in the vessel providing the O-ring seal, a cap was placed over the top. The cap has its center bored out so that it slides over the protruding third tier of the top. The ports in the top are left exposed while securing the cap and do not need to turn as the cap is screwed down onto the threaded vessel. Due to the weight of the cap and the size of the threads a superstructure was fabricated to give support for lifting the cap during set up and tear down of the system. The superstructure was made with aluminum extrusion pieces from 80/20 Incorporated due to their easy modular assembly and strength. A pulley system is attached to the superstructure for lifting the cap on and off the vessel system. HiP recommended that a copper-based lubricant is

applied to the vessel/cap threads to prevent seizure due to force from the high pressure and wear from assembling and disassembling the heavy cap.



Figure 23: Cap of the pressure vessel system with bore and threading shown

5.1.4 Sub Vessel

A flexible rubber sub vessel was designed specifically to meet the system needs of chemical compatibility, insulation, and flexibility. A mold of the correct size for our electrode assembly was created with special shape to accommodate an expansion chamber. The clay mold was wrapped in latex, and then spin coated in liquid rubber adding layers of rubber until the desired 1.5 mm thickness was achieved. The sub vessel was designed to hold the working fluid during electrolysis and to electrically insulate the electrolysis process from the pressurizing fluid and rest of the system. The sub vessel was also designed with an expansion chamber to accommodate gas production during the experiment without reducing the electrode's submersion in the electrolyte. The expanding chamber was added to the upper section of the vessel above the electrodes.

As the experiment continues and some of the electrolyte is changed into the gaseous products the upper chamber expands. The flexibility of the sub vessel allows the pressure throughout the system to stay equalized during the experiment. The placement of the expanding chamber ensures that submersion of the electrodes is not changed which would significantly alter the experimental results.



Figure 24: Flexible rubber diaphragm sub-vessel.

A size 13.5 rubber stopper was used to seal the container so that the working fluid would not mix freely with the pressurizing fluid. Three interference fit holes were drilled out of the stopper for the two electrical inputs and a mass flow system. The rubber stopper was frozen with liquid nitrogen and then machined in a lathe to have a lip where a pipe clamp could be used to seal the rubber sub vessel onto the rubber stopper. Note that the sub vessel is not designed to hold 5000 PSI just the slight difference in pressure that may occur during transient periods of the experiment between the sub vessel and the pressure vessel.

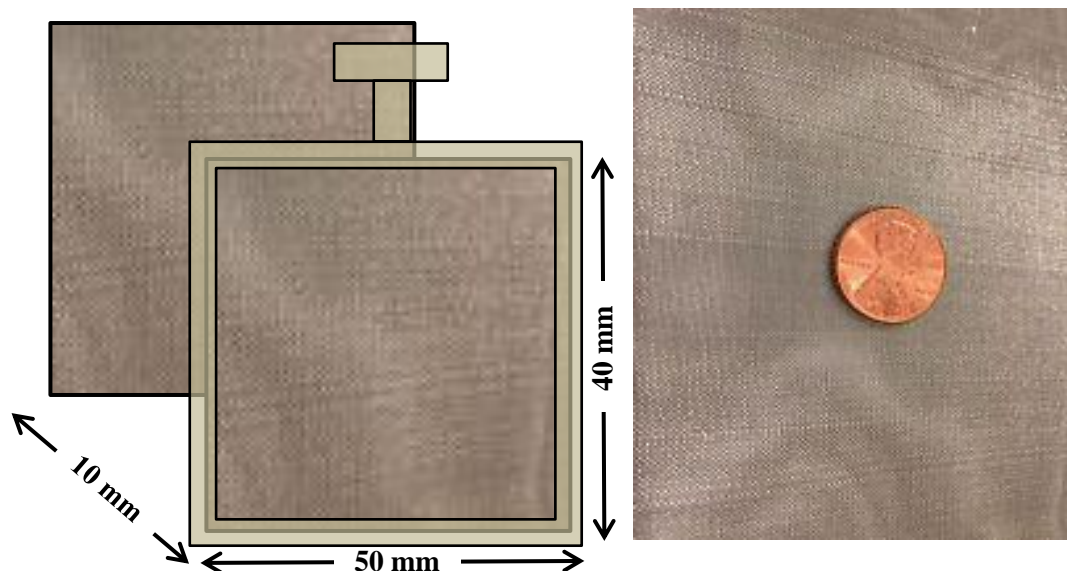


Figure 25: #60 Stainless mesh electrode geometry and size

A T-track system was designed and machined from polypropylene plastic and affixed to the rubber stopper using urethane based epoxy. The T-track provided an interference fit slot in which the electrode frames could slide providing the ability to set the electrode distance precisely. The frames were also machined from polypropylene plastic with a groove to accept the mesh electrode edges and a T to fit the track. The standard distance between the electrodes in further testing was set to 10 mm, however the range of the track was between .5 mm and approximately 5mm. The electrodes were made from a #60 stainless steel mesh which was the optimal mesh size for low pressure electrolysis suggested by literature (Zhang, Merrill et al. 2010). The electrodes had a length of 50 mm, a height of 40 mm, and the spacing between them was set at 10 mm.

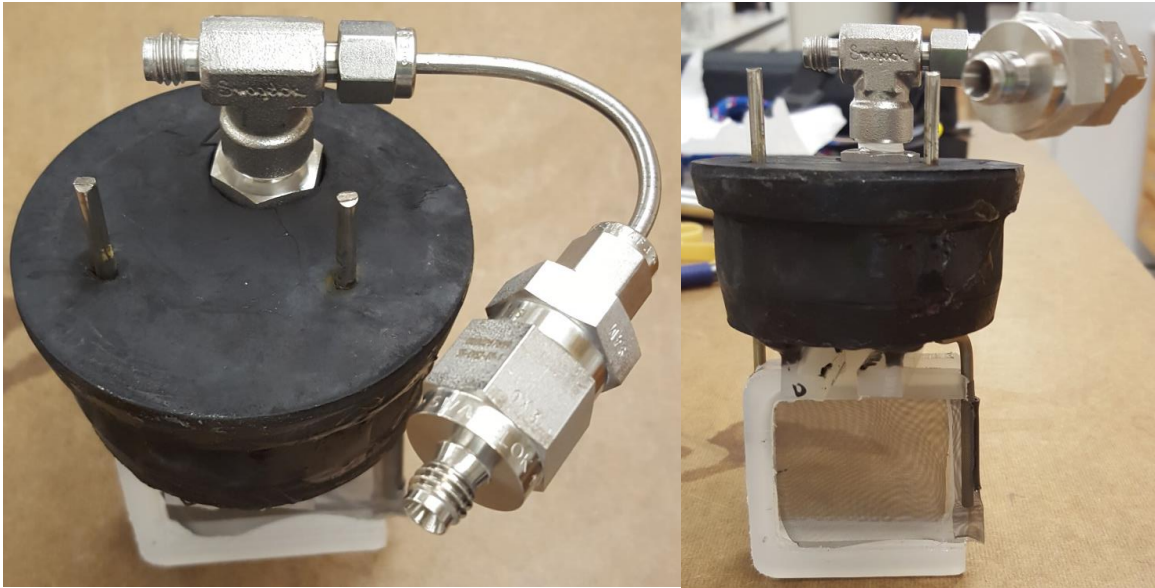


Figure 26: Rubber stopper with electrodes and outlet T-junction attached.

The mass flow system contains a T-junction with two one-way 5000 psi valves which keep the electrolyte and pressurizing fluid separate during pressurization and testing.

The perpendicular one-way valve allows the system to backfill the junction during pressurization so that it is not crushed. The in-line valve prevents the pressurizing fluid from entering the sub-vessel and contaminating the electrolyte. Potassium Hydroxide is selected as the electrolyte for its high conductivity and because it allows for direct comparison to low pressure scientific and industrial electrolyzers currently in operation. The electrolyte does not escape the sub-vessel because the one-way valve requires a 2 psi pressure difference to open. During pressurization the pressure vessel always maintains a slightly higher or equal pressure when compared to the sub vessel. As the pressure in the vessel increases the sub vessel is compressed slightly and the pressure equalizes.

When the testing is complete and the pressure in the vessel is released the sub-vessel momentarily has a higher pressure than the pressure vessel. This opens the one-way valve and allows the produced gas to be vented into the T-junction and out of the vessel. The gas and working fluid still do not escape into the pressure vessel because the perpendicular valve does not allow it. The sub vessel is connected directly to the exhaust port via a quick disconnect Swagelok fitting. This fitting is the direct link between the sub vessel and the exhaust port into the gas collection chamber outside the pressure vessel. This prevents any gas or electrolyzer fluid from contaminating the pressure vessel during experimentation.

5.1.5 Pump

To pressurize the system, an Eldex Optos model 2SM chemical metering pump was used. Optos metering pumps are specially designed for high-pressure applications with a range of different fluids. The Optos pump offered a max pressure of 6000 psi and a max flow rate of 10 mL/s.

5.2 Electrical System

A Keithley model 2440 is used to supply the electricity needed to perform electrolysis experiments. Its ability to record electrical data allows for accurate efficiency measurements when compared with produced gas. As discussed in section 5.1.2.3 electrodes were inserted through the top of the pressure vessel. They were sealed into the top using Conax glands and then passed through a #13.5 rubber stopper into the

sub-vessel. These electrodes carry the voltage into the sub-vessel where they are isolated from the pressurizing fluid inside the pressure vessel. Finally inside the sub-vessel the electrodes were connected to the anode and cathode, 4 cm by 5 cm rectangles of #60 316 stainless steel mesh. This specific mesh was chosen based on previous research highlighting its many geometrical advantages (Zhang, Merrill et al. 2010).

The simplified schematic of the pressure vessel system and the electrical system's place inside is shown in Fig. 22. Note that all parts of the pressure vessel system are color coded to blue.

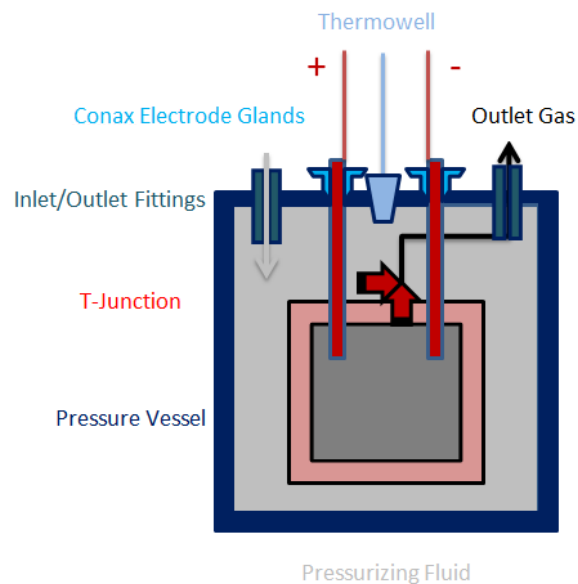


Figure 27: Schematic of pressure vessel with electrical sub system. Pressure system color coded to blue. Electrical Sysytem color coded to red.

5.3 Piping and flow system

The flow system was designed to pump the pressurizing fluid into the vessel until a target pressure was reached, and to retrieve product gases from within the reactor. An illustration of the flow system as a whole is shown in Fig. 23.

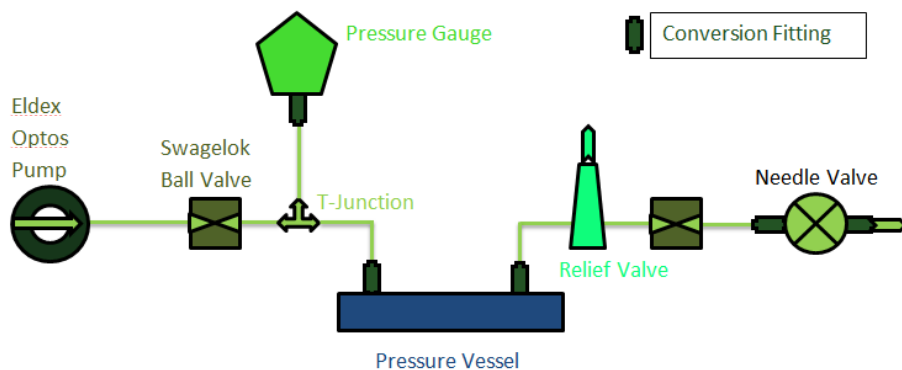


Figure 28: Diagram of flow system. Color coded to green.

As shown the flow system begins in the Eldex pump, Swagelok provided the appropriate modular 1/16 and 1/8 inch SS-T2-S-028-20 316 stainless steel tubing for our flow system. This tubing was chosen for its flexibility and strength allowing safe operation at 5000 psi. The flexibility of this tubing allowed it to connect all the components easily without the need for complex and expensive elbows or angle joints. In conjunction, Swagelok SS-200-7-4 316 stainless steel female connectors were used at each fitting point. Swagelok also provided the 316 stainless ball valves, model SS-4SKPS4 for 1/4 inch fittings which were used to isolate the system during testing reducing wear on the pump and needle valve. With the vessel, HiP supplied a pressure gauge (catalog serial number is 4PG10) designed for use up to 10,000 psi with marks every 100

psi. For safety, a relief valve attached immediately to the outlet of the pressure vessel was included in the flow system. The blowout valve supplied by HiP (catalog serial number HiP-10RV), is designed to release the pressure if it spikes above our safe operating pressure. Because most pieces in the system were rated to 6250 psi and our working pressure is 5000 psi, this valve acts as the emergency safety outlet if pressures exceed 5500 psi. Finally to control the flow out of the system, a high-sensitivity needle valve supplied by HiP (catalog serial number 30-11HF4) was used. The sensitivity of the needle valve allowed a safe slow release of produced gases which were measured by a flow meter or otherwise collected and then exhausted through a fume hood.

6. Experimental Procedures

6.1 Pressure safety testing

The first tests run on the apparatus were designed to test the safety of the vessel under high pressure. The secondary goal of these tests was to find and rectify any leaks or potential hazards relating to high pressure operation. The pressure vessel was filled with distilled water and the sub vessel was filled with dyed tap water. Distilled water is degassed for 15 minutes at -635torr before use in the pump to prevent cavitation which could damage the delicate sapphire and ruby piston. The piping and flow system is then connected and the vessel is sealed. The testing was started by pumping water through the system at the maximum flow rate with all valves open to flush any residual gas out of the vessel and piping system. Once a steady flow of water is seen with no gas, the needle valve and then the second ball valve are closed. The pump was then run at 1ml/min and the apparatus was monitored for leaks. After several tests the external leaks had been identified and rectified and no leakage of the dyed electrolyte fluid was detected in the pressurizing fluid.

6.2 Electrical safety testing

The next type of test performed on the apparatus was designed to test the safety of the electrical system. Following the same procedure as the pressure safety test the apparatus was set up and sealed. After flushing the residual gas out of the system the Keithley power source was turned on at 2 Volts. The compliance amperage was

restricted to 100mA to prevent possible injury by accidental shock. The system was then probed by a multimeter to test for any short circuiting through the vessel, superstructure, or piping system. Probing for short circuiting continued during the pressurization of the vessel to prove that safe operation could be achieved without the risk of shock at any pressure. It is important to note that prior to depressurization the electricity should be turned off or the flow outlet pipe could become charged. This condition will only occur if very small amount of gas is produced during testing. It is then possible for some of the electrolyte solution to foul the flow outlet pipe during depressurization. Although the plastic one-way valves and insulated interior piping attached to the "live" electrolysis sub-vessel should insulate the outlet piping in theory it is not recommended to run the apparatus in this way. If depressurization occurs and the electrolyte fouls the outlet line during live testing the circuit can be completed momentarily while the one-way valve is open, charging the outlet pipe and creating a shock hazard. The electrolyte fluid which could potentially foul the line would be too dilute to conduct a large amount of electricity, but it is better to follow procedure and prevent this occurrence. Following proper operating procedure and ending electrical testing before depressurization will protect the user from being in danger of shock even at high voltage.

6.3 Hydrogen Production Tests

To begin a test, the vessel is filled with distilled water for use as the pressurization fluid and as added insulation from the electrolysis. The majority of the vessel is filled with distilled water prior to closing the top so that only a small amount needs to be pumped into the system. This reduces set-up time as the pump's maximum flow rate is 10 mL/min and all gas must be expelled before testing. The electrolyte fluid must be produced prior to each test and is comprised of 10% by weight potassium hydroxide in distilled water. Some papers do not document their production of the electrolyte leaving the reader to guess at whether the solution was purchased already mixed or if they generated it themselves. Still others make the error of simply weighing the KOH sample and adding it to the whole quantity of water they desire not taking into account the solutions change in density or the water present in the KOH sample they use. In an effort to be more accurate when generating the proper weight percent solution this work considers the change in density of the final solution and approximates the weight of water present in the KOH sample. Using this information the weight of KOH pellets obtained from Sigma Aldrich as 85% KOH and 10-15% water with minor trace elements is calculated as 31.98 grams per 250 mL of solution. To safely produce this solution 200 mL of distilled water are added to a graduated Erlenmeyer flask. Then the KOH pellets are added slowly stirring them into solution while monitoring the temperature of the exothermic reaction between the two. Finally when all the pellets

have been added distilled water is added to the flash until the entire solution reaches 250mL. It is important to add the pellets to an ample amount of water slowly and not to add water to pellets as the reaction could boil the water sending caustic solution splattering. In this way we create the most accurate solution with little to no danger of injury. Next the electrolyte fluid is added to the sub vessel and the rubber stopper is sealed into place with the pipe clamp. The electrodes are connected to the electrical system and the Swagelok QC4-SS-400-SESO quick disconnect fixture is attached to the outlet port. This completes the electrical circuit and the flow system allowing the top and cap to be lowered into the vessel ready for testing. Approximately 250 mL of distilled water is degassed for 15 minutes at -635torr before use in the Optos 2SM pump to prevent cavitation which could damage the delicate sapphire and ruby piston. The piping and flow system is then connected via the Swagelok SS-200-7-4 fittings and seal the vessel. The process is started by pumping water through the system at the maximum flow rate with all valves open to flush any gas out of the vessel and piping system. Once a steady flow of water is seen with no gas, the HiP 30-11HF4 needle valve and then the second Swagelok SS-4SKPS4 ball valve are closed. The pump is run until reaching the desired pressure of 5000 psi. At this point the pump is paused and the first ball valve is closed isolating the system from the pump. Next the Keithley or other power source is connected to the electrodes and a desired input voltage is selected. The Keithley 2440 uses in-house software to control and measure its output. Our sample loop holds the

voltage steady for a desired test period allowing a maximum of 2000mA to be drawn by the system. During this time the voltage and amperage are recorded by the Keithley every 30 seconds. This allows us to monitor for any ramping in electrolysis or other inconsistencies during testing. It also provides the necessary data for calculating the efficiency of operation during any particular test. To capture the produced gas the outlet is connected to a two container liquid trap system filled with tap water. The ball and needle valves are then opened slowly allowing a safe flow rate of mixed pressurizing fluid and gas to escape into the container. The bottom of the first container has a one way valve which allows excess water to escape while the produced gases collect at the top of the container. The second container is open to the air and served only as a reservoir for excess water to escape into during depressurization. After the pressure is released from the vessel the pump is turned back on and run for 2 minutes at maximum flow rate to make sure all the product gases are flushed out of the system and collected in the container. The amount of gas produced is measured and recorded to compare to the electricity used by the Keithley in order to determine the efficiency of the system. During the first tests a sample of the product gas was passed into a 7890A Agilent gas chromatograph (GC) to check that produced gas was the desired hydrogen and oxygen mixture. During all tests a Sperian Biosystems Toxil TD meter is used to monitor for leaks of hydrogen gas and all product gases are vented directly to the fume hood.

7 Results and Discussion

7.1 System Design

The first accomplishment of this work was the design and fabrication of a 5000 psi working pressure electrolysis system. Initial pressure and electrical safety testing proved the design's robustness and ability to sustain electrolysis reactions at any pressure between 0 and 5000 psi. Data associated with safety testing is available but not presented here. This system which includes the pressure vessel, piping and flow system, pressure control devices, electrical subsystem, and integrated safety devices cost approximately 20,000 dollars. The magnitude of this achievement is highlighted by the extreme cost of the only known units capable of operation at this pressure created by industry leaders at a cost more than 2 million dollars each over 5 years. Our system, which was designed to be as simple and flexible as possible, allows future electrolysis testing to be conducted with many variables changed so the behavior of high pressure electrolysis can be studied. The main reason for designing a high pressure electrolysis system is to prove that the efficiency gains of high pressure electrolysis are substantial as compared to a low pressure setup with compression. A second major benefit of this flexible system is the ability to study and characterize the behavior of electrolysis systems with regards to changes in variables such as electrolyte concentration, conductivity, electrode geometry and spacing, and system efficiency with large pressure changes.

7.2 Tap Water Testing

7.2.1 Stability Testing

Preliminary testing and characterization of our high-pressure electrolyzer was completed using tap water as the electrolyte and a high input voltage. This configuration was chosen primarily to test the unit's repeatability and robustness at 5000 psi before introducing more caustic electrolytes. Preliminary studies also sought to prove long-term stability and robustness of the system during hours of continuous operation seen in Fig. 25. While tap water is far from an ideal electrolyte it was exceedingly safe to use when first testing a system newly constructed at very high pressures.

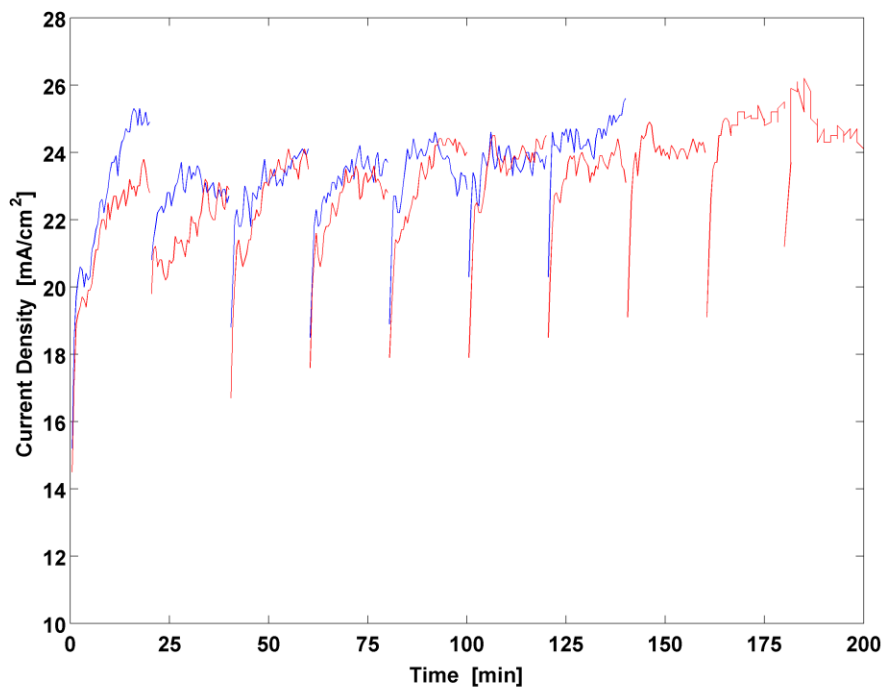


Figure 29: Current density over time during 20 minute intervals testing at 40 V

Gas samples were extracted every 20 minutes to determine production rate of product gases over time. Data collected from these two separate tests shows that each time the electric power is turned off and back on, an electrical activation period during which very little gas is produced occurs. This activation period is relatively short and production over time is relatively stable. Multiple tests in excess of 120 minutes were performed and repeatability of testing was confirmed even over long time periods. A slight increase in the current density was observed over time during the extended tests as seen in Fig. 26. This increase is likely attributed to the reaction of trace elements in the Durham city tap water with the steel mesh electrodes or with themselves.

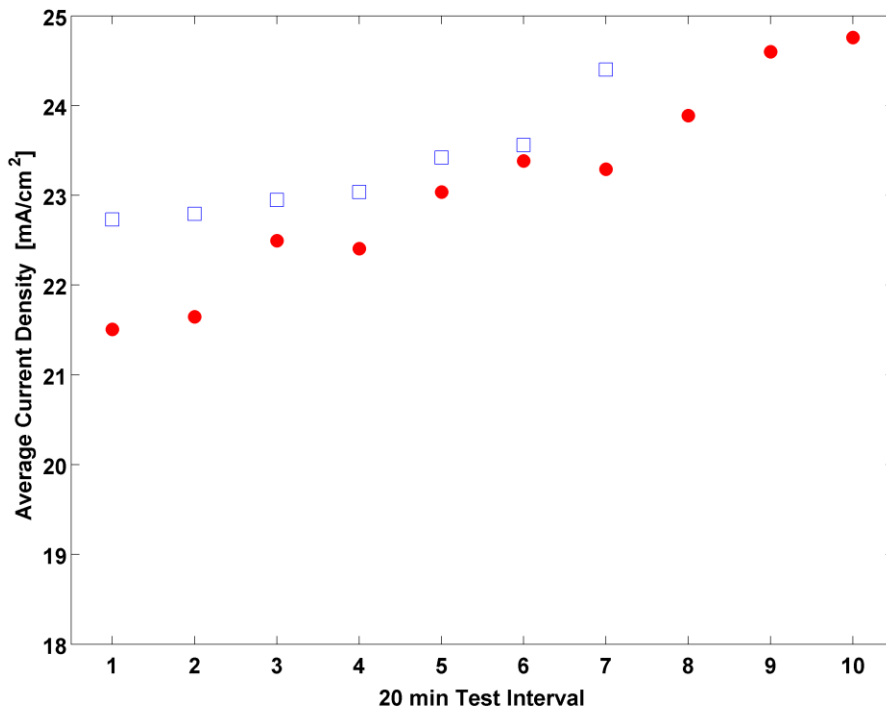


Figure 30: Current density averaged over all 20 minute intervals.

Physical evidence of this occurrence was perceived in three ways. The first way was the observation of very small, unexpected peaks in gas chromatograph measurements of the product gas. This indicates the presence of unknown trace gases in the product mixture. The second hint was the small amounts of orange precipitate in the reaction chamber after extended testing. The final observation was that slight degradation of the steel mesh electrodes, which occurred after many hours of testing were performed. It is assumed that tests performed with a distilled water/KOH solution will show reduced activation periods and better stability. Volumetric gas production rates for each 20 minute interval were recorded during both extended testing and multiple one hour test periods. The average gas production rates for each interval are shown in Fig. 27.

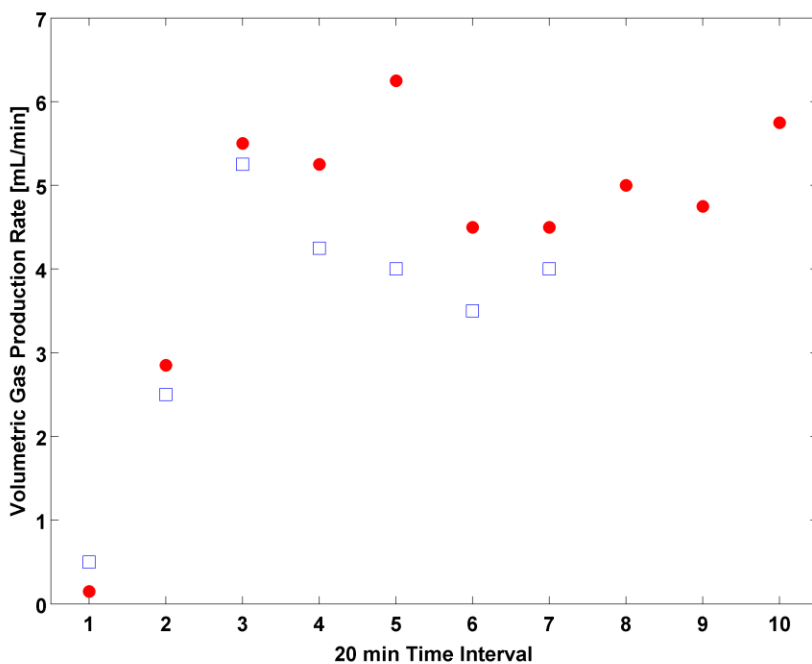


Figure 31: Volumetric gas production rate for all intervals.

Note that the first two intervals of any test have a low gas production rate. It is hypothesized that this phenomena is attributed to the reaction of trace elements in the tap water. During this time very little gas is produced because the energy supplied is used on the reaction of trace elements and not for the desired reaction of water splitting. After the second interval, however, gas production stabilizes and remains relatively constant over time.

7.2.2 Pressure Variation

Since the testing showed that the system produced stable results over long time periods, 1 hour tests were chosen for further characterization, beginning at 1000 psi up to the target pressure of 5000 psi. Since the conductivity of the tap water electrolyte is poor, and increased gas production for measurement purposes was required, 40 V with a compliance of 1 A was used for these tests. During testing the current density was monitored and is shown below in Figs. 28 – 32, averaged for four tests at each pressure over time. Also included on the graphs is the \pm standard deviation (σ) for the average taken over the 4 independent runs with time. For all pressures, after approximately 10 min or less, very stable current densities are observed. There is relatively little difference in current density with varying pressure, which supports the thermodynamic claims that increased pressure will at first increase cell voltage significantly but after 1500 PSI it will level off.

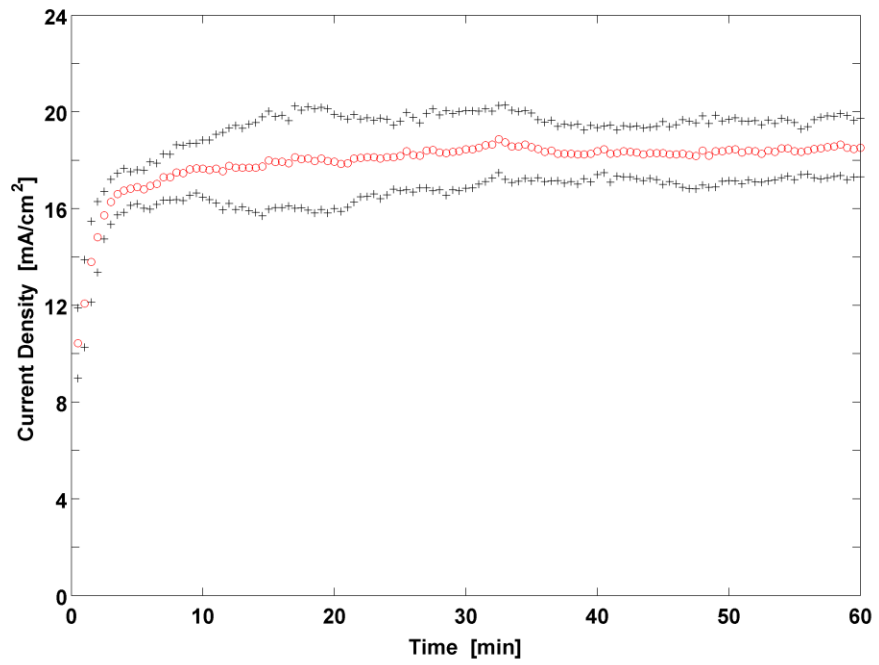


Figure 32: Average current density and average $\pm \sigma$ over time for 4 tests at 1000 psi

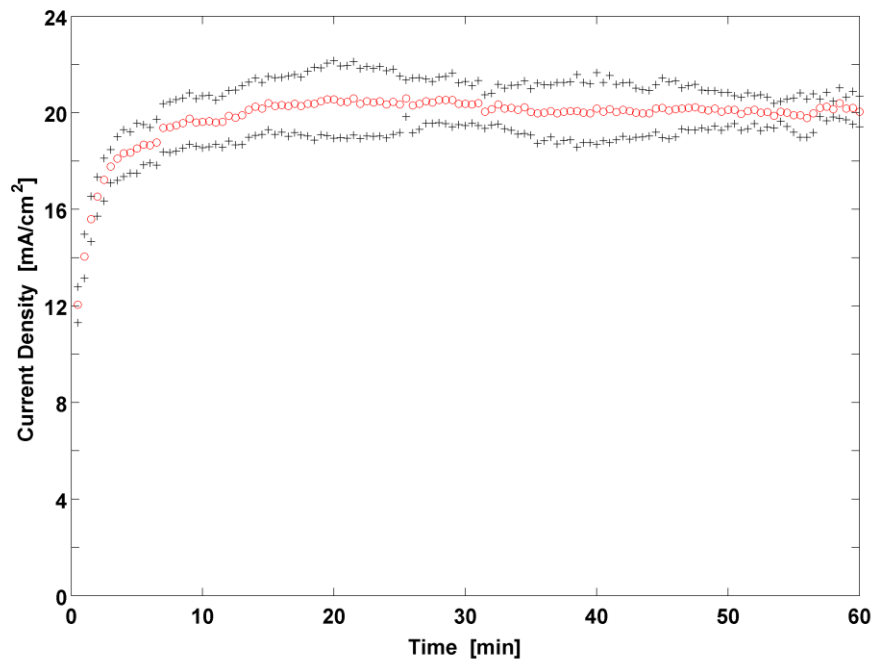


Figure 33: Average current density and average $\pm \sigma$ over time for 4 tests at 2000 psi

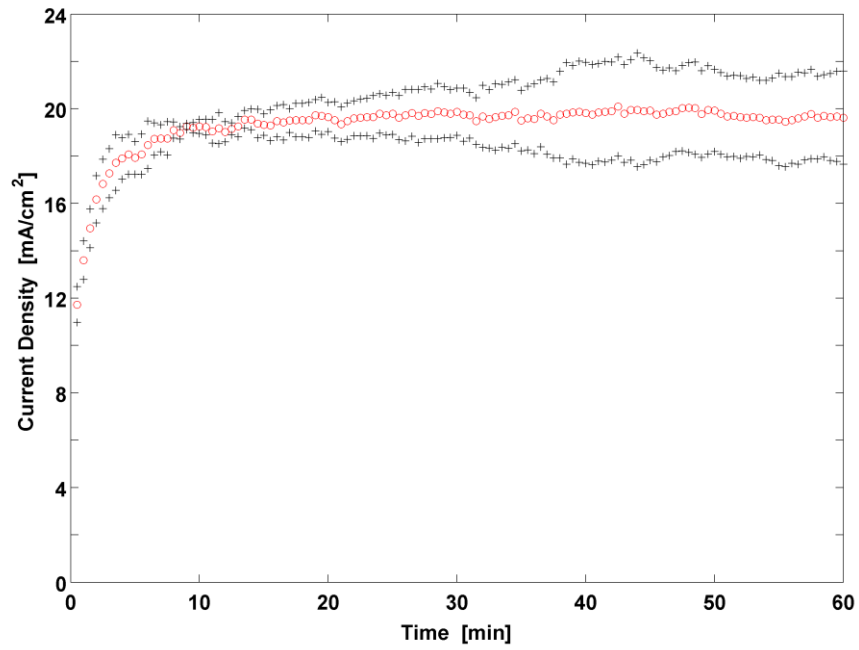


Figure 34: Average current density and average $\pm \sigma$ over time for 4 tests at 3000 psi

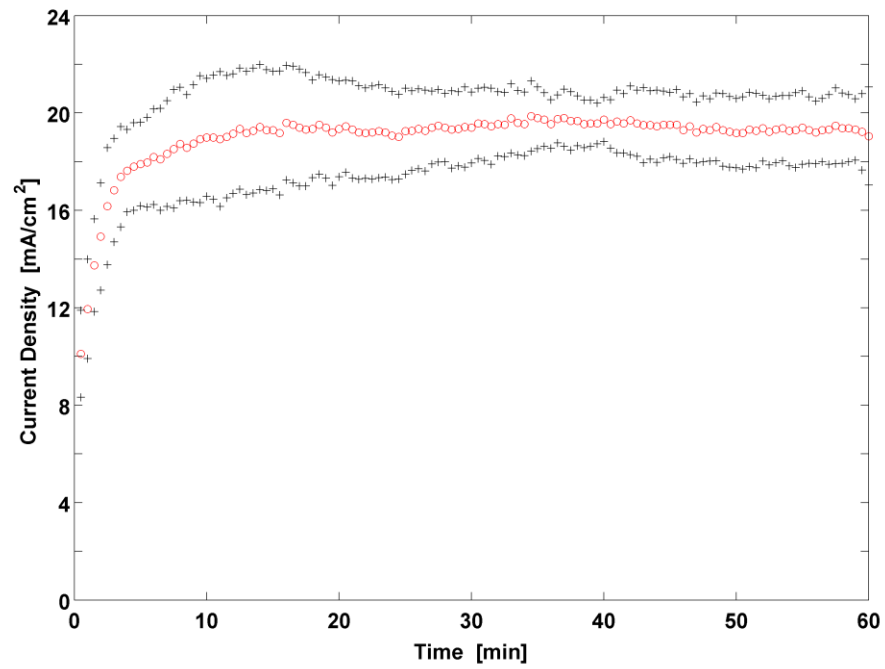


Figure 35: Average current density and average $\pm \sigma$ over time for 4 tests at 4000 psi

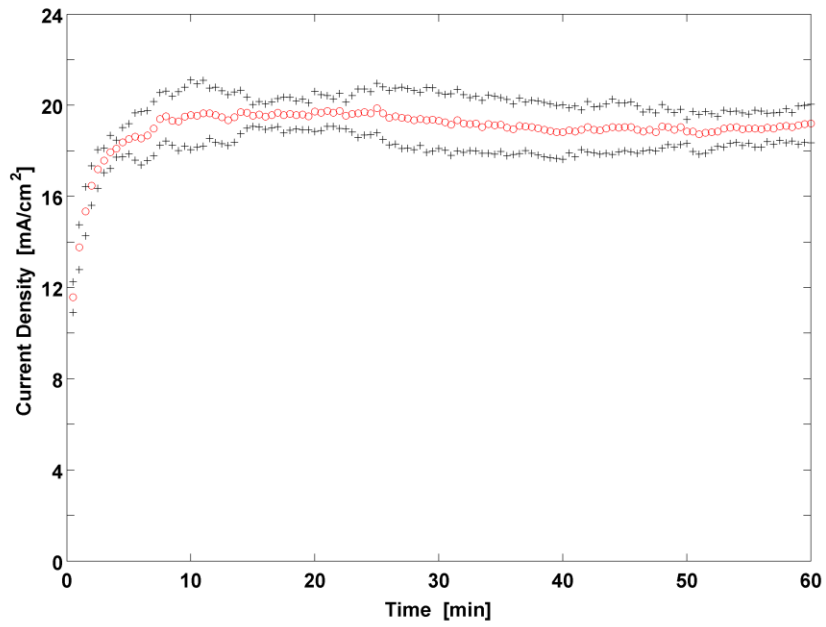


Figure 36: Average current density and average $\pm \sigma$ over time for 4 tests at 5000 psi

Figure 33 shows the average current density of all tests performed at each pressure.

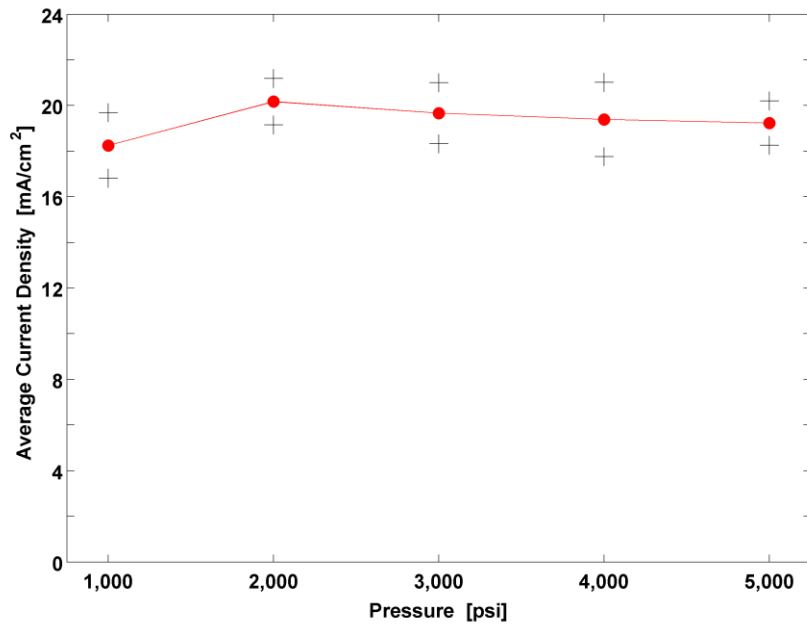


Figure 37: Average current density and average $\pm \sigma$ at each pressure

Theoretically a slight increase in the power required for electrolysis at each pressure should be observed. Our data shows a slight increase from 1000 psi to 2000 psi and then a very slow decrease for higher pressures up to 5000 psi. This data is somewhat inconclusive because the overall variance in current density is only twice the standard deviation. We believe that a more conductive electrolyte will create a more accurate testing environment, allowing this subtle change to be measured.

7.2.3 Voltage Variation

After confirming that the system was capable of operation at a range of pressures for extended periods of time the next logical step was to improve its efficiency by lowering the electrolysis voltage. As the system voltage approaches the thermo-neutral voltage, which is approximately 1.48 V (Leroy, Bowden et al. 1980, Onda, Kyakuno et al. 2004), the efficiency of the system rises. Since the target pressure of the system is 5000 psi all voltage tests were done at this pressure. For the sake of direct comparison to previous testing, voltage tests were performed for one hour at the target pressure starting at 40 V. Although the tap water electrolyte is poor and therefore the system efficiency very low, it was hoped that a change in efficiency would still be perceived. Voltage test were done at 40, 30, 20, 10, and 5 V with the intention of continuing down to the theoretical thermo-neutral voltage, however, no gas was produced at 5 V. Future testing with the suggested KOH electrolyte is expected to produce far more favorable results and should be capable of producing results below 5 V. Figure 34 shows the

current density averaged over 4 runs for 40 V and 1 run each for the other voltages, all results starting at 10 min run time after the activation period.

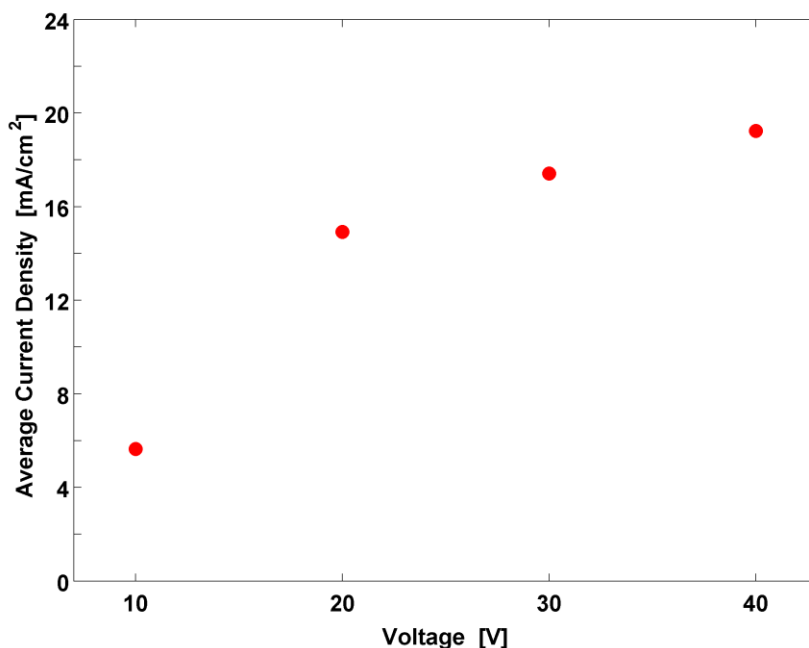


Figure 38: Average current density observed during testing at each voltage

As expected the current density driven across the poor electrolyte is bolstered by higher voltages. The required current density increases strongly for lower voltages and less significantly for higher voltages. Finally, below 10 V the production goes to zero as there is not enough voltage to drive the reaction. In order to maximize gas production and efficiency an ideal system will lower its operating voltage while retaining current density. In other words the limiting factor in the reaction should be current density. This would allow us to lower the voltage, improving system efficiency without sacrificing gas production. If current density were the limiting factor, the graph would show a

relatively constant current density across a range of voltages. With the current apparatus and tap water electrolyte, the observed current density increases with voltage and, therefore, voltage is still the limiting factor. Since voltage is the limiting factor in our system, the gas production increases linearly with increased voltage, which is shown in Fig. 35.

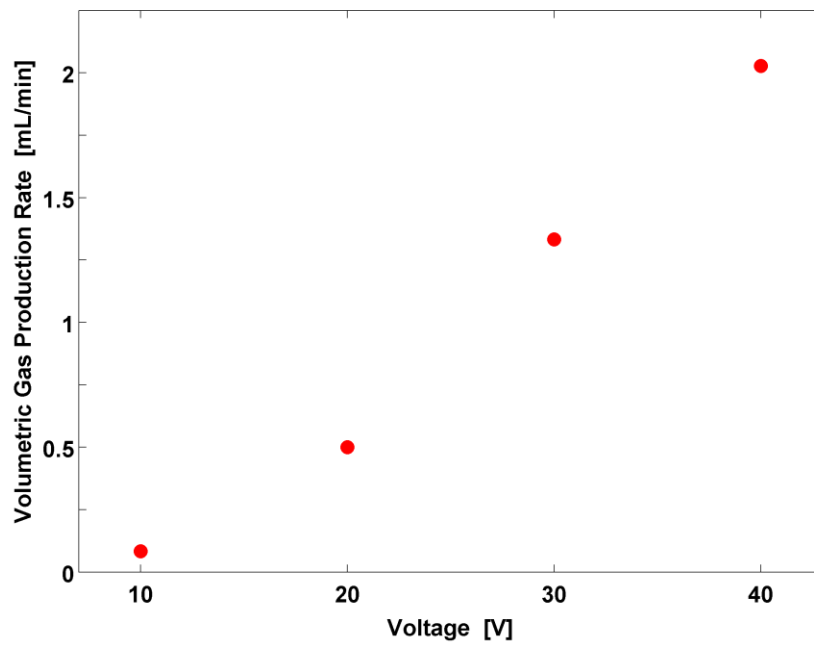


Figure 39: Volumetric gas production at different voltages.

7.3 Potassium Hydroxide Testing

7.3.1 Potassium Hydroxide Concentration Variation

The final design of the system calls for the use of a highly caustic potassium hydroxide electrolyte similar to the ones typically used in industrial electrolyzers. The new KOH electrolyte not only allows for a more direct comparison to current low pressure hydrogen electrolyzers but should also increase the efficiency of the system dramatically. Various concentrations of KOH are used as an electrolyte for hydrogen generation in both industry and literature. In order to select a concentration for detailed testing in our system a wide range of concentrations were tested to show their effects on gas generation and efficiency. The first step was to determine at ambient pressure, the effect of changes in KOH concentration on the minimum electrolysis voltage and maximum voltage as set by amperage limits imposed by our safety standards. By performing a voltage sweep from 1 to 5 V in different concentrations of electrolyte we identified the range of voltages to be used in further testing. Figure 36 shows the swept voltages vs the recorded current in electrolytes with a 1, 10, 20, and 30% weight solution of KOH in distilled water. The effect of increasing the concentration of KOH is a marked improvement in the current which can flow through the solution at each voltage. The increased concentration of KOH in the electrolyte considerably lowers ohmic losses in the system by increase in the conductivity of the electrolyte. However the increase in conductivity is logarithmic in nature, so continually increasing the concentration of

KOH will eventually yield little to no improvement in the solutions ability to carry more current(Opu 2015). Although increasing the KOH concentration to its saturation point of approximately 45% by weight would provide the highest possible efficiency most industrial units use a 30% weight solution. This is due to the harsh caustic nature of the electrolyte and the reduced efficiency gains at the highest concentrations. For detailed testing we choose to use a maximum concentration of 10% by weight for safety reasons. At this concentration if electrolyte were to leak from the 250mL sub vessel the 5 liters of pressurizing fluid would reach ~0.1 molar concentration. This would be relatively safe to clean up and would not affect the stainless steel vessel in any way.

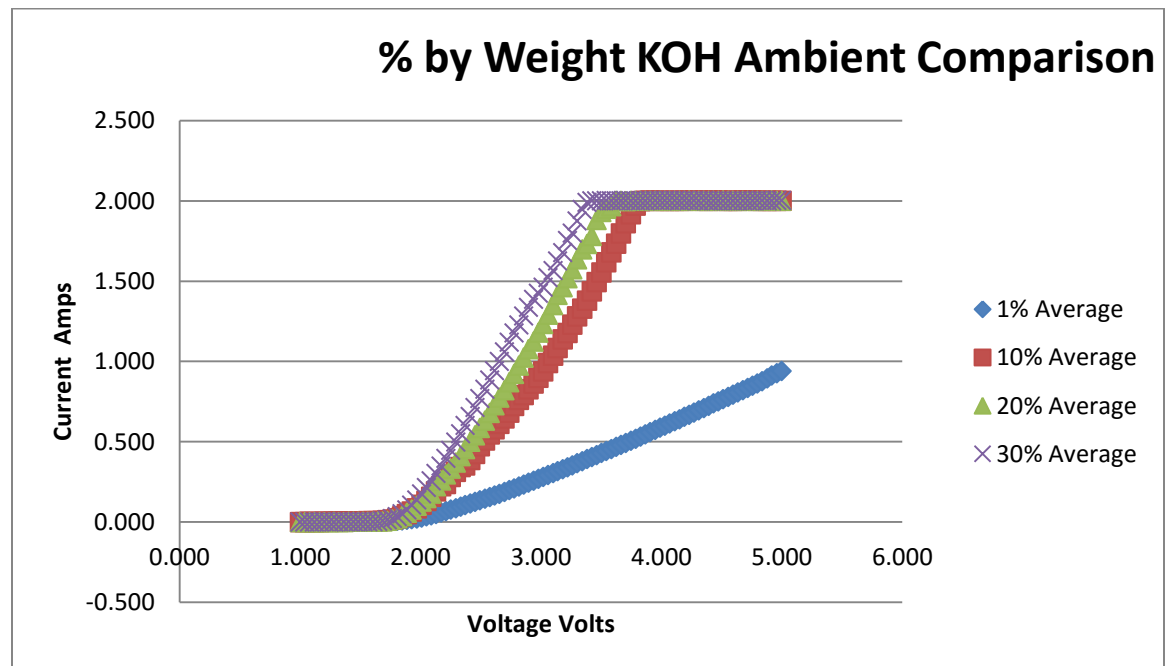


Figure 40: Effect of KOH concentration on current observed from 1-5 V

The sweep test allowed us to determine the range of interesting voltages for future testing would be between 1.75 and 3.0 V, the approximate minimum voltage at which

electrolysis was observed in the system, and the maximum voltage at which the amperage limit was exceeded. Since these tests are performed at ambient pressure the flow system remains open and we can observe bubbles created by electrolysis as soon as they are created. The sweep testing also indicated approximate values for the thermo-neutral voltage of our system at different concentrations of KOH electrolyte. During the sweep test the voltage and amperage at which bubbles were first observed was marked. This data provided confirmation that bubble formation began in between 20 and 30mA of total current. This region of the graph is the area where the current begins to increase non-linearly and finally reaches a constant linear progression with increasing voltage. This area of interest from figure 36 is presented enhanced in figure 37.

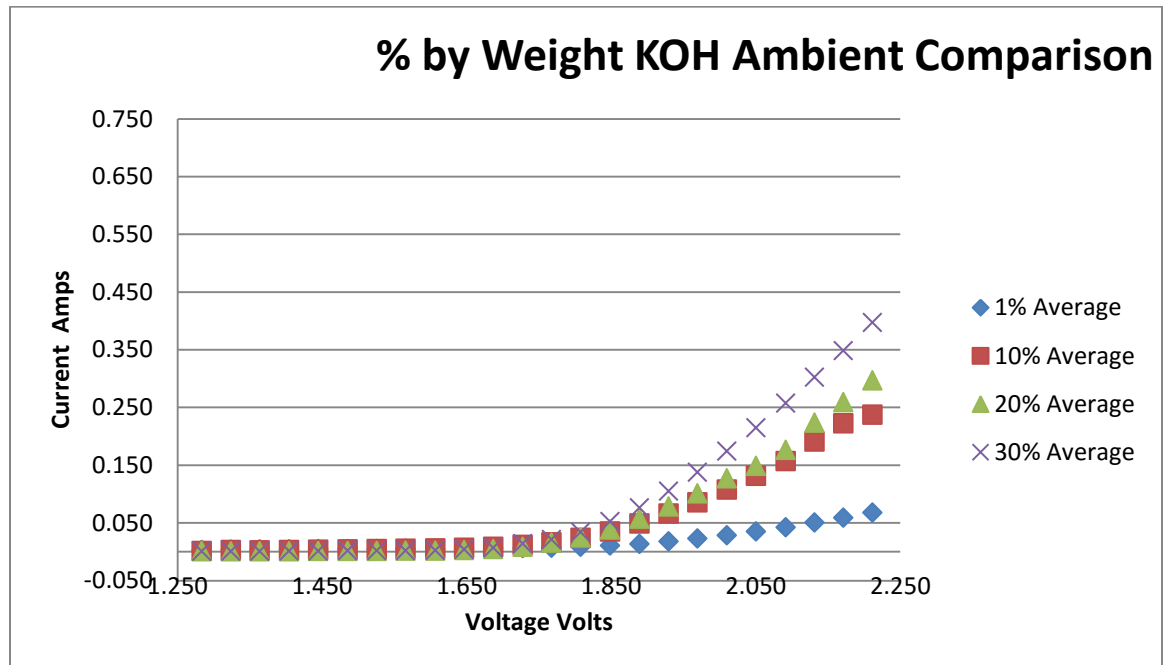


Figure 41: Effect of KOH concentration on current observed from 1.25-2.25 V

This indicates that the nonlinear section of the graph is the system overcoming the over voltages predicted in figure 12 and finally beginning production after which the loss of efficiency is mainly caused by increased ohmic loss with increasing voltage. It is encouraging to note that our system produces hydrogen using a voltage of approximately 1.75 volts. This voltage is in line with the minimum cell voltage of current low pressure state of the art technology and well below typical industry cell voltage of 1.9-2.25 volts. Figure 38 shows the TSEL system's minimum cell voltage as compared to the theoretical minimum cell voltage for electrolysis (Onda, Kyakuno et al. 2004), cell voltage of current state of the art low pressure electrolyzers (Zeng and Zhang 2010), and cell voltage of typical industrial electrolyzers (Cropley and Norman 2008). Note that the theoretical minimum cell voltage calculated as ~1.48 do not include over voltages. In a real system hydrogen and oxygen evolution over voltages and cathode/electrode over voltages are present and so achieving this theoretical cell voltage is impossible.

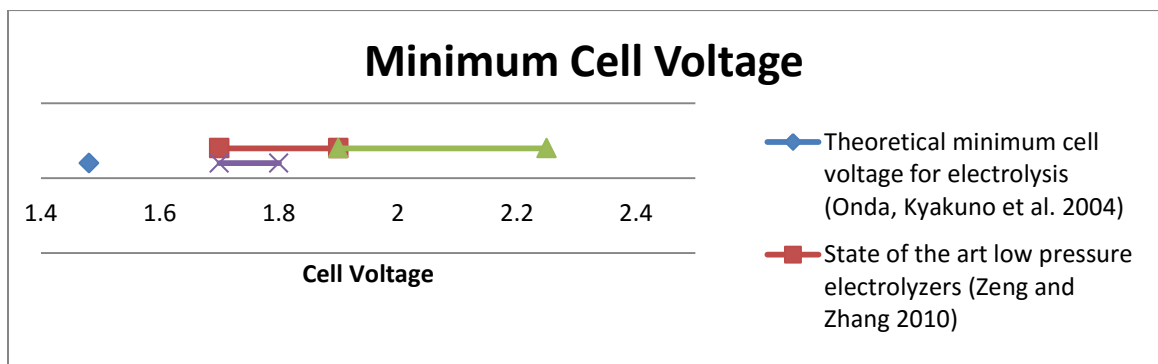


Figure 42: Cell Voltage For Electrolysis

Following the initial sweep testing, in depth analysis of the efficiency and gas production at target voltages in different concentrations of KOH was conducted. Based on the sweep data voltages between 1.75 and 3.0 volts were selected and gas production tests were run to analyze the systems efficiency.

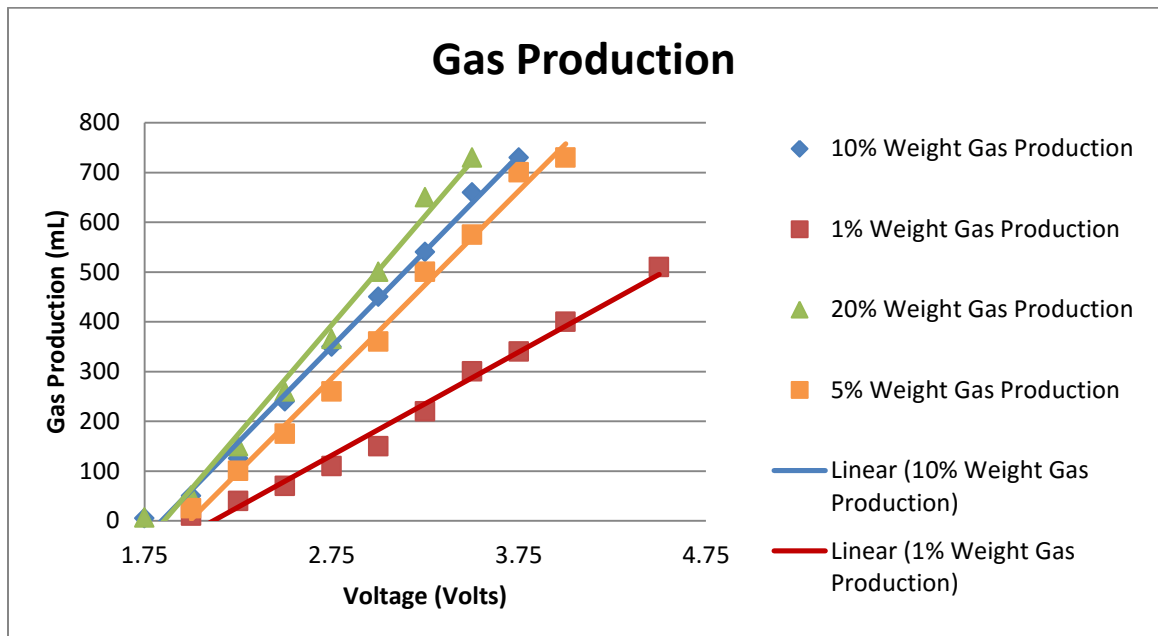


Figure 43: Gas production at different voltages and KOH concentrations

Figure 39 shows the results of increasing the voltage used for electrolysis in the selected concentrations of KOH electrolyte. As expected the gas production increases linearly with the increase in voltage until it reaches the imposed maximum of approximately 720 mL of gas. This limit is imposed by the safety procedures of our tests and system which limits the total applied amperage to 2 A. At this time the system becomes artificially limited in terms of current density by the power source instead of by the electrolyte solution's ability to transfer charge. Study of the behavior outside this artificial limit is

possible but is outside the scope of this work. Limiting the study to lower voltages is not only for the safe operation of the system however. This is because high voltages and currents cause greater ohmic losses and reduce the system efficiency to unacceptable levels. Even though higher voltages allow for better gas production rates they can cut the efficiency of the system in half from ~80 to 40%.

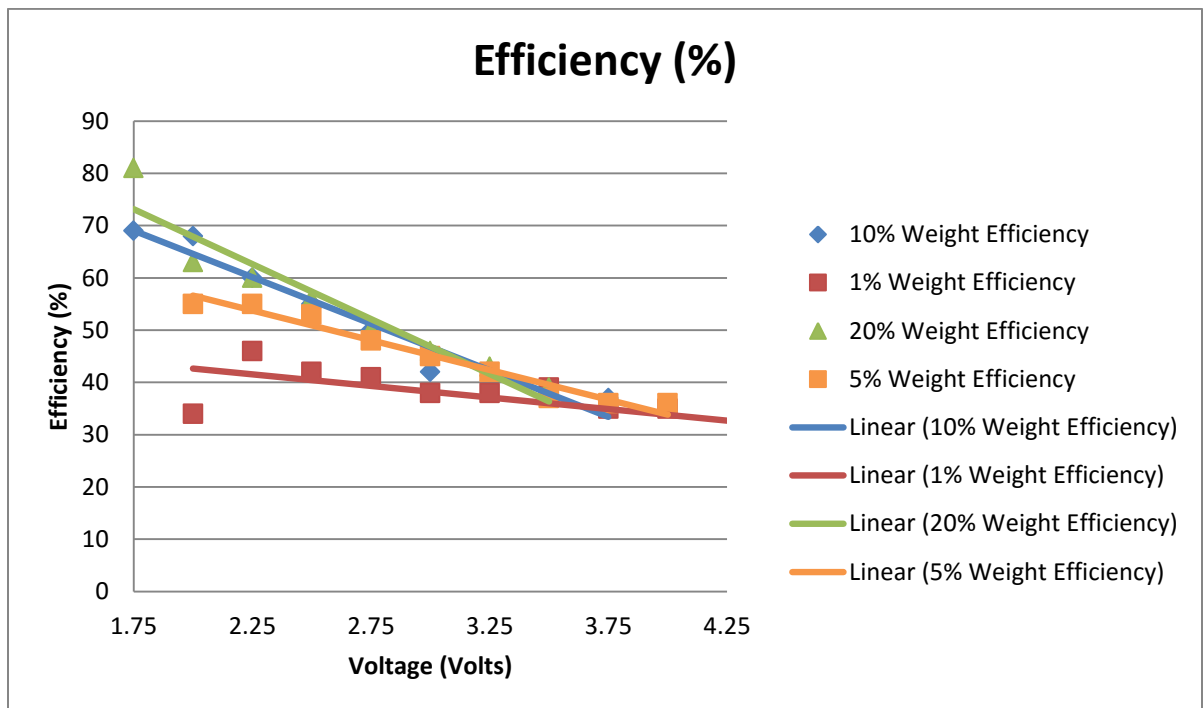


Figure 44: Efficiency of electrolysis vs. voltages at selected KOH concentration

Figure 40 depicts the relationship between voltage and electrolysis efficiency in the selected KOH concentrations in our system. As predicted electrolysis efficiency is highest at low voltages near the reversible electrolysis voltage and at high KOH concentrations. Here the ohmic losses are small and the efficiency of our system was

recorded as high as 86%. This number corresponds almost exactly with values in literature for low pressure electrolysis that states the efficiency of a cell operating at 1.75 V as 85.6 % (Leroy, Bowden et al. 1980). As the voltage is increased the efficiency of the electrolysis process decreases linearly. This is mainly an expression of the greatest loss in the system the ohmic loss. Ohmic loss will increase linearly with increased voltage and current density at all concentrations of electrolyte. For the 1% and 5% weight concentrations the lowest voltages tested 1.75 and 2.0 V, the gas production was too small to be accurately measured by our apparatus. However the remaining data can be used to extrapolate reasonably, and the trend across different concentrations of KOH electrolyte is still clear. After reviewing the efficiency and gas production of the system and keeping in mind safety we choose 10% weight as the concentration for further study in the system. This concentration provided a good balance of safety, cost effective use of KOH, and good electrolysis efficiency in the system.

7.3.2 Pressure Variation

Current theoretical literature suggests that increasing the pressure of the environment in which electrolysis takes place should cause a small increase in electrolysis voltage between 0 and 1500 psi. However at pressures above 3000psi very little change in electrolysis voltage is predicted as shown in figure 11. The main goal of the TSEL system was to be the first to produce data in this high to ultrahigh pressure regime. This will not only serve as a way to verify current theoretical analysis but will

also further the field of high pressure alkaline electrolysis by providing a versatile platform for high pressure electrolysis experimentation. With the safety of the TSEL system verified, the new sub vessel completed, and the KOH concentration selected, pressure testing was started to determine the effect of pressure on electrolysis in the system. A range of cell voltages were tested and the current densities achieved as well as gas production rates were recorded across a range of pressures. Data was collected at 2.0, 2.5, and 3.0 volts at ambient pressure and then at 1000, 2000, 3000, 4000, and 5000 PSI. Figure 42 and 43 show two visualizations of how pressure affects current density (kA/m²) in the system at the selected cell voltages.

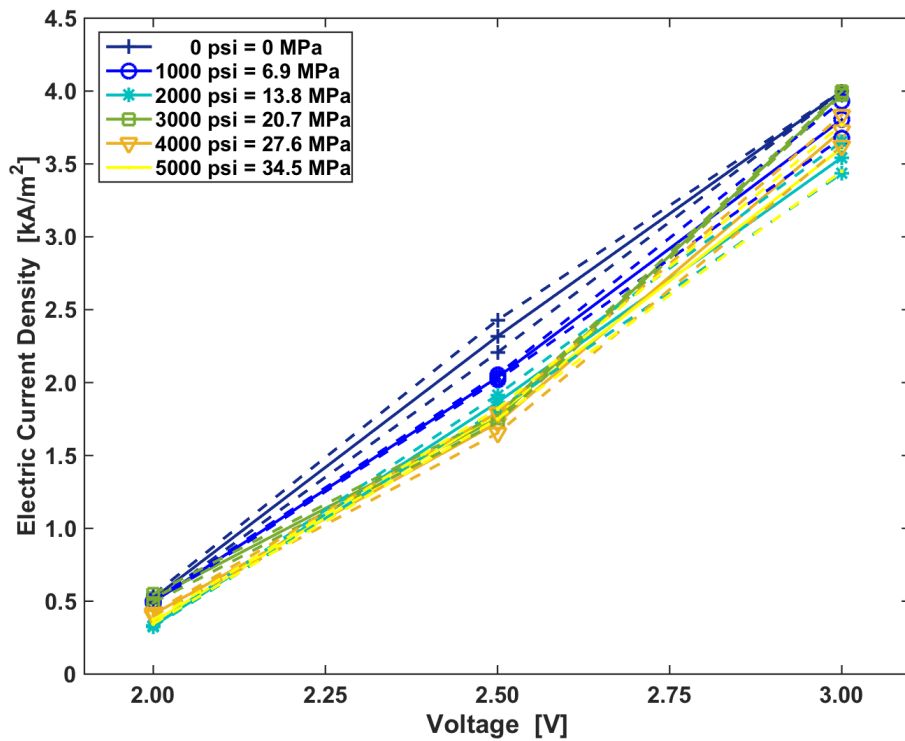


Figure 45: Effect of pressure change on electrolysis current density

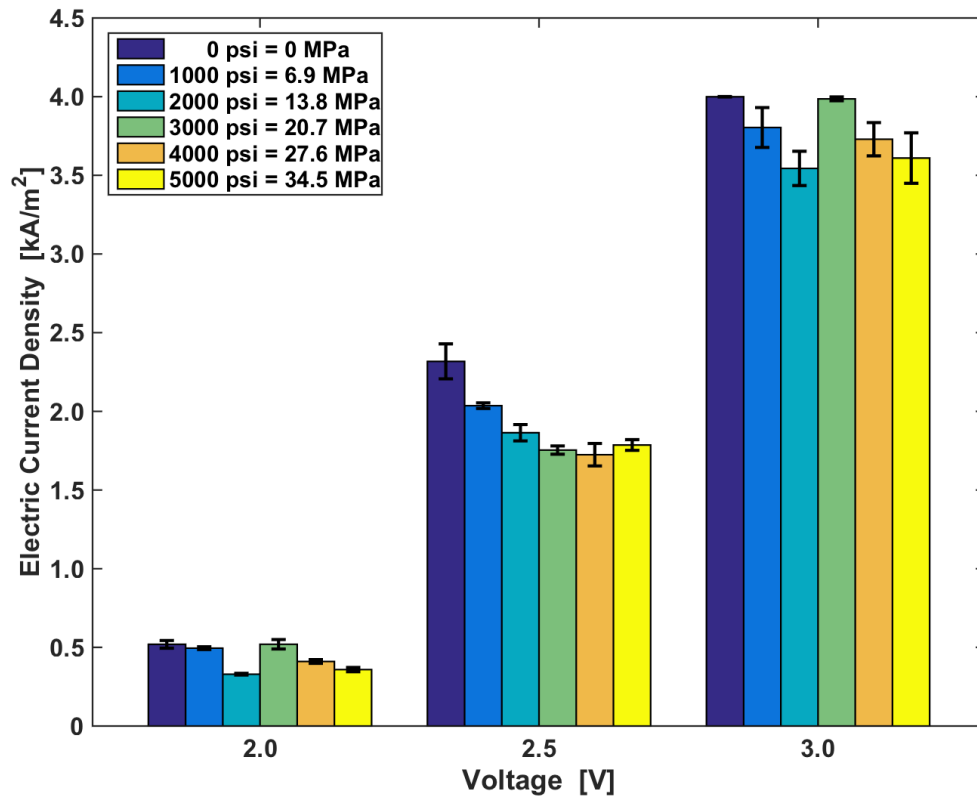


Figure 46: Effect of pressure change on electrolysis current density

It is clear that at ambient pressure the systems current density is highest at all voltages when compared to the current density of the system at increased pressures. Although it is not perfect, the other trend that seems to emerge in the data is that with increased pressure there is initially a significant reduction in current density but a reduced effect is seen as the pressure increases. It is impossible to observe gas production due to the nature of the high pressure environment in which the electrolysis takes place. However one possible explanation for the decrease in current density is an increased masking effect produced by slow moving bubbles created at the electrodes. As the pressure in the

system increases the radius of the bubbles created during electrolysis decreases. These smaller bubbles rise more slowly than larger bubbles making masking at higher pressure more pronounced and reducing the conductivity of the solution surrounding the electrodes. This hypothesis could be confirmed by changing the electrode geometry or by experimenting with forced convection of the solution in order to carry produced bubbles away from the electrodes faster. Next we examine the effect of pressure on gas production rate using two similar visualizations in figures 44 and 45.

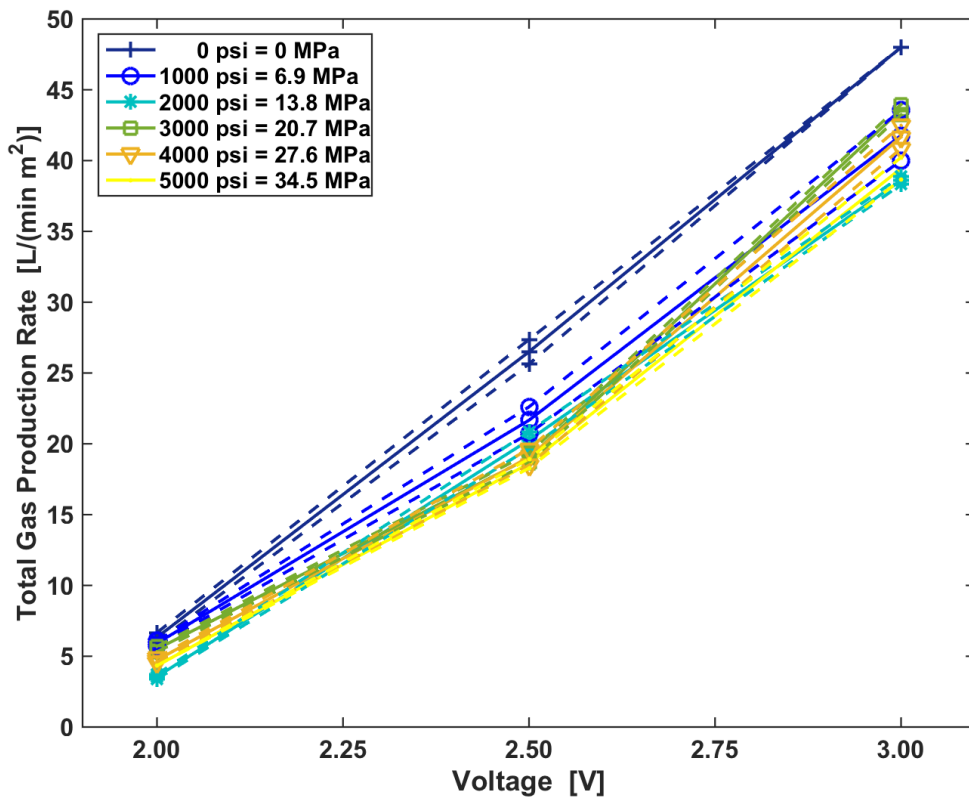


Figure 47: Effect of pressure change on gas production

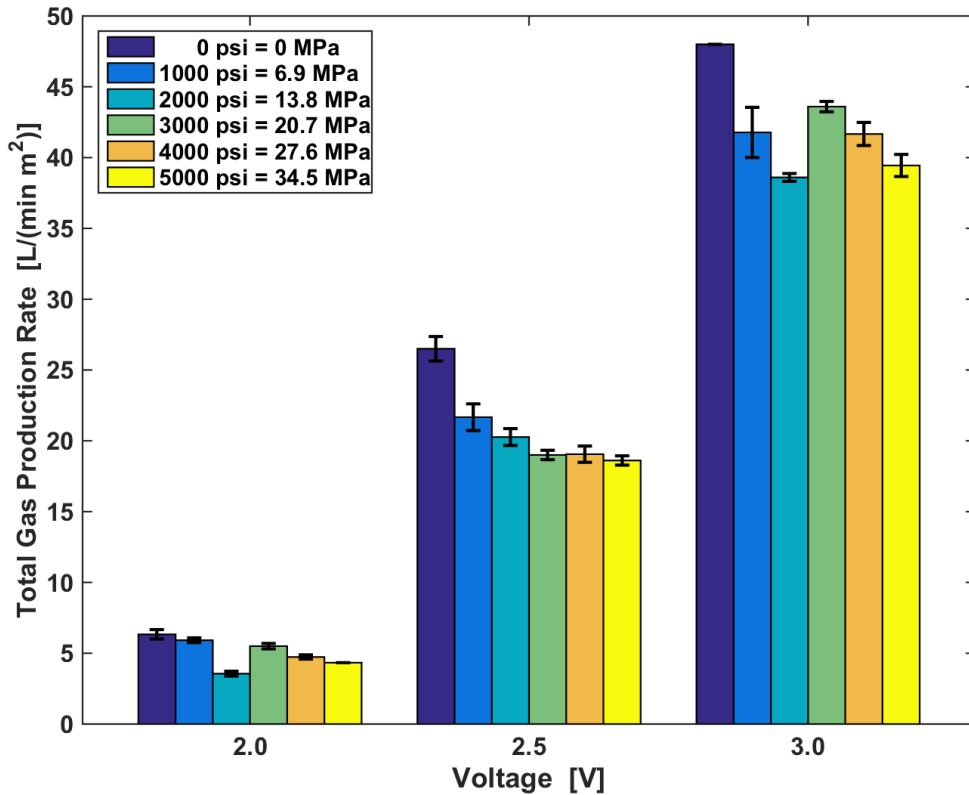


Figure 48: Effect of pressure change on gas production

As predicted based on the current density data a similar trend in gas production versus system pressure is observed with the highest rate occurring in the ambient pressure system. Again a slight reduction in production rate is seen over the range of increased pressures which is expected since the current density and gas production rate are directly linked. A decoupling of current density and gas production rate data would have suggested that the increase in pressure had significantly altered one of the other resistances to gas production and that it was the limiting factor in the TSEL system. While (Tsiplakides 2016) did hypothesize that a significant increase in pressure should

decrease the resistance of mass transport at or very near the electrodes we do not see this effect in our system. This along with the coupled gas production and current density data suggest that conductivity in the electrolyte solution is the limiting factor in the TSEL system. Experimental analysis of ionic conductivity vs pressure also suggests that the conductivity of the solution will decrease at very high pressures (Parveen Kumar 2007). While initially a small increase in conductivity is observed with rising pressure a maximum is reached near 1500 psi at which point ionic conductivity decreases with increasing pressure. This is another possible explanation for the slight reduction in performance of the TSEL system at ultrahigh pressure. This explanation supports the observed decrease in current density and gas production. Verification of this effect could be observed by running a test at constant voltage during which the pressure is gradually increased and the current density and gas production are monitored over time. Finally we plot the systems efficiency calculated as the electrical energy input to the system by the Keithley divided by the energy contained in the produced hydrogen gas (LHV) using equation 4. This data is presented in figures 46 and 47 for the target voltages and pressures in a visualization matched to the gas production and current density graphs for continuity. The efficiency data in figure 46 shows the expected trend of decreasing efficiency with increased cell voltage however a trend across increased pressure is less obvious.

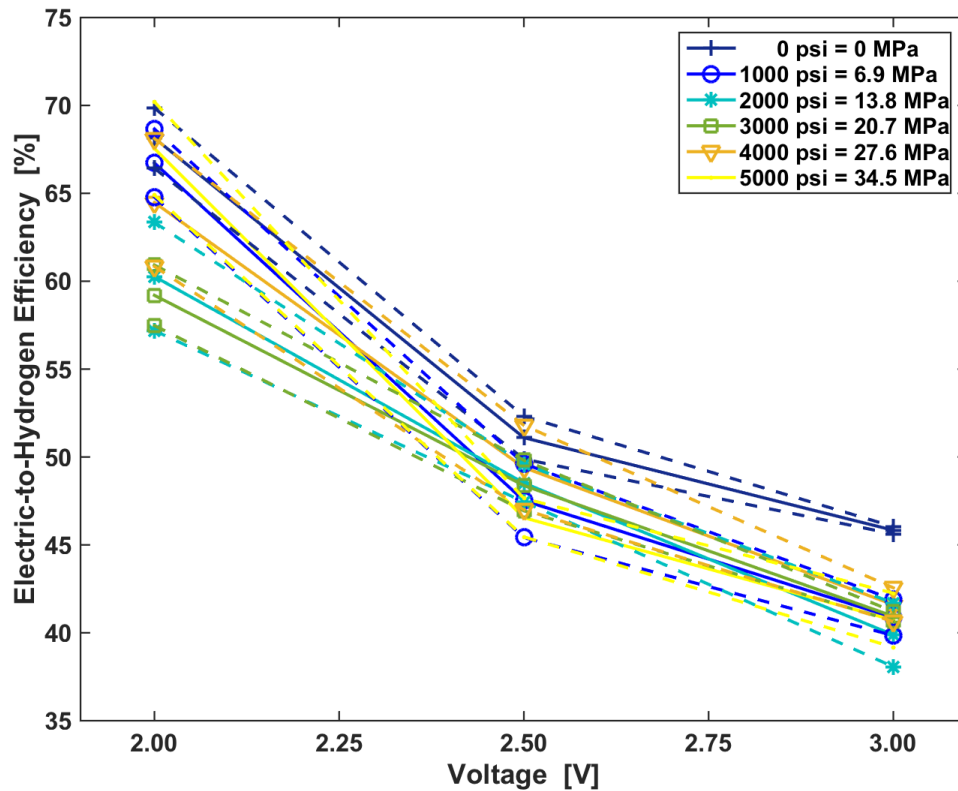


Figure 49: Effect of pressure change on system efficiency

In figure 47 the effect of pressure on the system’s efficiency is more clear, and indicates that the efficiency of the system is slightly higher at ambient pressure but is relatively unchanged at higher pressures. Current thermodynamic theory suggests that the cell voltage needed for electrolysis will rise significantly from 0 to 1500 psi but will then level off as pressure increases (Onda, Kyakuno et al. 2004, Laoun 2007, Todd, Schwager et al. 2014). If we consider that cell voltage is directly linked to ohmic losses the system efficiency should therefore follow a similar trend. This trend becomes an important consideration when comparing low and high pressure electrolysis systems.

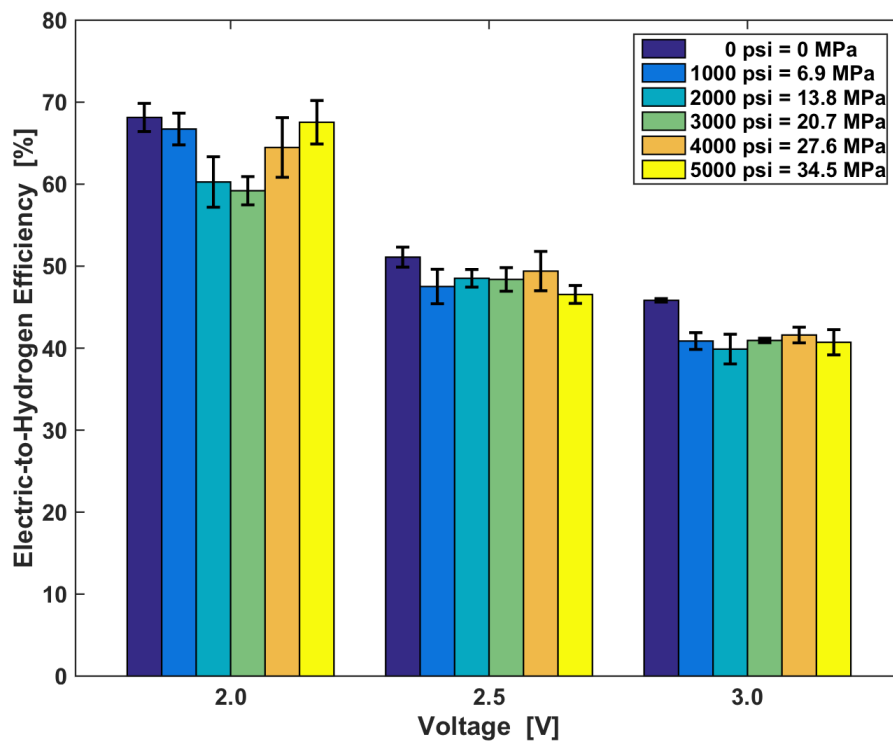


Figure 50: Effect of pressure change on system efficiency

It also supports the theory from current literature that cell voltage initially increases with pressure but eventually levels off. To further prove this increase in cell voltage which is predicted by current literature the system could be run at the target pressures while sweeping across voltages between 1.48 V the theoretical minimum, and approximately 2.0 volts where the system shows ample gas production. By monitoring current during these sweeps and comparing it to the minimum current at which gas production begins in the TSEL system approximately 30 mA a minimum cell voltage for electrolysis could be estimated at each pressure.

Finally in figure 48 we present the comparison of TSEL’s low cost versatile ultra high pressure system to the current state of the art in alkaline electrolysis. It is important to note that the efficiency of our system is competitive with other scientific and industry systems despite its extremely low cost, reduced electrolyte concentration, and low tech electrodes. It is likely that with more advanced electrodes and a stronger electrolyte the TSEL system could meet or exceed the current state of the art low pressure systems and produce gas at ultrahigh pressures which other systems can’t reach.

Parameter	De Nora SAP	Norsk Hydro	Electrolyzer Corp Ltd	Teledyne	Force Tech	Duke TSEL	Duke TSEL	Industry
Electrodes	Ni-plated steel	Activated Ni-coated steel	Ni-coated steel	Ni-Screen	Raney Nickle	Steel Mesh	Steel Mesh	Ti/Ni Steel Mesh
Pressure MPa	Ambient	Ambient	Ambient	0.2	3	Ambient	34.47	3
Temperature °C	80	80	70	82	100	24	24	80
Electrolyte	29% KOH	25% KOH	28% KOH	35% KOH	25% KOH	10% KOH	10% KOH	20-40% KOH or NaOH
Current Density kA/m²	1.5	1.75	1.34	2.0	2.0	0.5-2.3	0.3-1.75	0.2-0.4
Cell Voltage V	1.85	1.75	1.9	1.9	1.68	2.0-2.5	2.0-2.5	1.8-2.4
Efficiency	nr	nr	nr	nr	88	52-68	48-68	40-60
Reference	(Zeng and Zhang 2010)			(Lars Yde 2013)			(Holladay, Hu et al. 2009)	

Table 3: Current state of the art Alkaline Electrolysis vs TSEL system

8 Conclusion

We have successfully designed a robust and versatile system for ultra-high pressure electrolysis. The system's structural integrity and safety has been extensively reviewed and is of sufficient quality for continued testing at pressures up to 5000 psi. UHP electrolysis studies have been conducted proving the systems stability during long term testing and repeatability. Pressure variation tests have shown that the systems efficiency will not be significantly lowered by large increases in pressure, which is in line with current literature and thermodynamic theory. Voltage variation tests showed the extent of the tap water electrolytes weakness as a conductor. This data proved that the conductivity of the solution was the limiting factor in a tap water system and therefore no further efficiency could be gained without the use of a stronger electrolyte. During all tests an activation period where no gas is produced was observed. These activation periods were undesirable due to their low gas production and a limited understanding of the reactions occurring during that time. In order to avoid the issues involving activation periods and current density limitations a 10% weight solution of distilled water and KOH was used. KOH is selected as the electrolyte over other similar electrolytes such as NaOH because it is more conductive in solution. While typical industrial electrolyzers use a 30% by weight aqueous solution of potassium hydroxide (KOH) in distilled water our testing was conducted using a 10% by weight solution. This was based on its performance, the cost of KOH, and the safety when considering a leak

into the main pressure vessel. The KOH electrolyte effectively removed the activation period from all test and provided a much better comparison to current industrial best practices and most scientific literature. Leak-free operation was achieved providing confidence for testing with caustic electrolytes such as the selected 10% weight KOH solution.

References

- A-F.M. Mahrous, I. M. S., A. Balabel, K. Ibrahim (2011). "Experimental Investigation of the Operating Parameters Affecting Hydrogen Production Process through Alkaline Water Electrolysis." International Journal of Thermal and Environmental Engineering 2(2): 113-116.
- Abbott, D. (2010). Keeping the Energy Debate Clean: How Do We Supply the World's Energy Needs? Proceedings of the IEEE. 98.
- Appleby, A. J., et al. (1978). "High Efficiency Water Electrolysis In Alkaline Solution." International Journal of Hydrogen Energy 3: 21-37.
- Armaroli, N. and V. Balzani (2011). "The hydrogen issue." ChemSusChem 4(1): 21-36.
- Ball, M. and M. Wietschel, Eds. (2009). The Hydrogen Economy, Cambridge University Press.
- Bossel, U. (2006). Does A Hydrogen Economy Make Sense. Proceedings of the IEEE.
- Brise, A., et al. (2008). "High temperature water electrolysis in solid oxide cells." International Journal of Hydrogen Energy 33(20): 5375-5382.
- Caspersen, M. and J. B. Kirkegaard (2012). "Modelling electrolyte conductivity in a water electrolyzer cell." International Journal of Hydrogen Energy 37(9): 7436-7441.
- Chen, L. and A. Lasia (1991). "Study of the Kinetics of Hydrogen Evolution Reaction on Nickel-Zinc Alloy Electrodes." Journal of the Electrochemical Society 138(11): 3321-3328.
- Conax (2014). "Packing Gland Diagram." from <http://www.conaxtechnologies.com/details.aspx?cid=PG&pid=PG>.
- Crnkovic, F. C., et al. (2004). "Electrochemical and morphological studies of electrodeposited Ni-Fe-Mo-Zn alloys tailored for water electrolysis." International Journal of Hydrogen Energy 29: 249-254.
- Cropley, C. and T. Norman (2008). A Low-Cost High-Pressure Hydrogen Generator, Department Of Energy.

Deretsky, Z. (2012). "Microbial Electrolysis Cell." Retrieved December, 2014, from https://www.nsf.gov/news/mmg/mmg_disp.jsp?med_id=66454&from=.

Dunn, P. and D. Maurterer (2011). High-Capacity, High Pressure Electrolysis System with Renewable Power Sources Avalence/DOE PP. Avalence Research and Development, Department Of Energy.

EERE (2014). "Hydrogen Production." from <http://energy.gov/eere/fuelcells/hydrogen-production>.

Energy, D. O. (2011). "2011 Annual Merit Review Proceedings." Retrieved 1/2012, 2012, from http://www.hydrogen.energy.gov/annual_review13_proceedings.html.

Fan, C., et al. (1994). "Study of Electrodeposited Nickel-Molybdenum, Nickel-Tungsten, Cobalt-Molybdenum, and Cobalt-Tungsten as Hydrogen Electrodes in Alkaline Water Electrolysis." Journal of the Electrochemical Society **141**(2): 382-387.

Frank Allebrod, P. L. M., Christodolus Chatzchristodolou, Mogens Mogensen (2011). ELECTRICAL CONDUCTIVITY MEASUREMENTS OF AQUEOUS AND IMMOBILIZED POTASSIUM HYDROXIDE International Conference on Hydrogen Production. Thessalonki Greece. **181**.

Ganley, J. C. (2009). "High temperature and pressure alkaline electrolysis." International Journal of Hydrogen Energy **34**: 3604-3611.

GREET, A. N. L. (2010). "The Greenhouse Gases, Regulated Emissions, and Energy Use in Transportation Model GREET." from <https://greet.es.anl.gov/>.

Hamdan, M. (2008). Low Cost High Pressure Hydrogen Generator. Giner Electrochemical Systems, Department Of Energy.

Hamdan, M. and T. Norman (2013). PEM Electrolyzer Incorporating An Advanced Low-Cost Membrane. Giner Electrochemical Systems, Department Of Energy.

Holladay, J. D., et al. (2009). "An overview of hydrogen production technologies." Catalysis Today **139**(4): 244-260.

IPCC (2007). "Fourth Assesment Report IPCC." 2014, from http://www.ipcc.ch/publications_and_data/publications_and_data_reports.shtml#1.

- Janssen, H. (2004). "Safety-related studies on hydrogen production in high-pressure electrolyzers." International Journal of Hydrogen Energy **29**(7): 759-770.
- Kelly, N. A., et al. (2008). "A solar-powered, high-efficiency hydrogen fueling system using high-pressure electrolysis of water: Design and initial results." International Journal of Hydrogen Energy **33**: 2747-2764.
- Kelly, N. A., et al. (2011). "Generation of high-pressure hydrogen for fuel cell electric vehicles using photovoltaic-powered water electrolysis." International Journal of Hydrogen Energy **36**: 15803-15825.
- Khaselev, O. and J. A. Turner (1998). "A Monolithic Photovoltaic-Photoelectrochemical Device for Hydrogen Production via Water Splitting." American Association for the Advancement of Science **280**: 425-427.
- Laoun, B. (2007). "Thermodynamics aspect of high pressure hydrogen production by water electrolysis." Review Of Renewable Energy **10**(3): 435-444.
- Lars Yde, C. K. K., Frank Allebrod, Mogens Bjerg Mogensen, Per Moller, Lisbeth R Hilbert, Peter Tommy Nielson, Troels Mathieson, Jorgen Jenson, Lars Anderson, Alexander Dierking (2013). 2nd Generation Alkaline Electrolysis. Mechanical Engineering Technical University of Denmark.
- Leroy, R. L., et al. (1980). "The Thermodynamics of Aqueous Water Electrolysis." Electrochemical Science and Technology.
- Logan, B. E., et al. (2008). Microbial Electrolysis Cells for High Yield Hydrogen Gas Production from Organic Matter. H. E. C. P. S. University.
- Marangio, F., et al. (2009). "Theoretical model and experimental analysis of a high pressure PEM water electrolyser for hydrogen production." International Journal of Hydrogen Energy **34**(3): 1143-1158.
- Marinia, S., et al. (2012). "Advanced alkaline water electrolysis." Electrochimica Acta **82**: 384-391.
- Milbrandt, A. and M. Mann (2007). Potential for Hydrogen Production from Key Renewable Resources in the United States NREL.gov, National Renewable Energy Laboratory.

- Moran, M. J. and H. N. Shapiro (2008). Engineering Thermodynamics, Wiley.
- Nagai, N., et al. (2003). "Existence of optimum space between electrodes on hydrogen production by water electrolysis." International Journal of Hydrogen Energy **28**: 35-41.
- NOAA (2010). "State Of the Climate." National Climatic Data Center. 2014, from <http://www.ncdc.noaa.gov/>.
- Norbeck, J. M., et al. (1996). Hydrogen Fuel for Surface Transport. Warrendale PA, Society of Automotive Engineers.
- Ohata, T. (2009). Energy Carriers and Conversion Systems. Oxford, UK, Eolss publishers.
- Onda, K., et al. (2004). "Prediction of production power for high-pressure hydrogen by high-pressure water electrolysis." Journal of Power Sources **132**(1-2): 64-70.
- Opu, M. S. (2015). "Effect Of Operating Parameter on Alkaline Electrolysis." International Journal of Thermal and Environmental Engineering **9**(2): 53-60.
- Parveen Kumar, A. K. S., S Yashoneth (2007). "Relationship between Ionic Radius and Pressure Dependence of Ionic Conductivity in Water." Diffusion Fundamentals **6**.
- R.J. Gilliam, J. W. G., D.W. Kirk, S.J. Thorpe (2007). "A review of specific conductivities of potassium hydroxide solutions for various concentrations and temperatures." International Journal of Hydrogen Energy **32**: 359-364.
- Shafiee, S. and E. Topal (2009). "When will fossil fuel reserves be diminished?" Energy Policy **37**(1): 181-189.
- Spurgeon, J. M. and N. S. Lewis (2011). "Proton exchange membrane electrolysis sustained by water vapor." Energy & Environmental Science **4**(8): 2993.
- Tao, G. and A. Virkar (2006). A Reversible Planar Solid Oxide Fuel A Reversible Planar Solid Oxide Fuel-Fed Electrolysis Cell and Solid Oxide Fuel Cell for Electrolysis Cell and Solid Oxide Fuel Cell for Hydrogen and Electricity Production Operating Hydrogen and

Electricity Production Operating on Natural Gas/Biogas on Natural Gas/Biogas,
Department Of Energy.

Thomas, G. and J. Keller (2003). Hydrogen Storage Overview.

Todd, D., et al. (2014). "Thermodynamics of high-temperature, high-pressure water electrolysis." Journal of Power Sources **269**: 424-429.

Toyota (2015). "Patent Release."

Tsiplakides, D. (2016). Water Electrolysis Fundamentals. D. o. Energy. DOE.gov, DOE.

Ulleberg, O. (2003). "Modeling of advanced alkaline electrolyzers: a system simulation approach." International Journal of Hydrogen Energy **28**: 21-23.

Willauer, H. D. (2010). Synfuel from Seawater. 2010 Naval Research Laboratory Review.
NRL: 153-154.

Zeng, K. and D. Zhang (2010). "Recent progress in alkaline water electrolysis for hydrogen production and applications." Progress in Energy and Combustion Science **36**(3): 307-326.

Zhang, H., et al. (2010). "Evaluation and calculation on the efficiency of a water electrolysis system for hydrogen production." International Journal of Hydrogen Energy **35**(20): 10851-10858.

Zhang, Y., et al. (2010). "The use and optimization of stainless steel mesh cathodes in microbial electrolysis cells." International Journal of Hydrogen Energy **35**(21): 12020-12028.